arXiv:0812.0057v3 [math.AP] 6 Nov 2009

A model for unsteady mixed flows in non uniform closed water pipes and a well-balanced finite volume scheme

Christian Bourdarias*, Mehmet Ersoy† and Stéphane Gerbi‡

Laboratoire de Mathématiques, Université de Savoie
73376 Le Bourget du Lac, France

Abstract

We present the derivation of a new unidirectional model for unsteady mixed flows in non uniform closed water pipes. We introduce a local reference frame to take into account the local perturbation caused by the changes of section and slope. Then an asymptotic analysis is performed to obtain a model for free surface flows and another one for pressurized flows. By coupling these models through the transition points by the use of a common set of variables and a suitable pressure law, we obtain a simple formulation called PFS-model close to the shallow water equations with source terms. It takes into account the changes of section and the slope variation in a continuous way through transition points. Transition point between the two types of flows is treated as a free boundary associated to a discontinuity of the gradient of pressure. The numerical simulation is performed by making use of a Roe-like finite volume scheme that we adapted to take into account geometrical source terms in the convection matrix. Finally some numerical tests are presented.

Keywords : Shallow water, mixed flows, free surface flows, pressurized flows, curvilinear transformation, asymptotic analysis, VFRoe scheme, well-balanced finite volume scheme, hyperbolic system with source terms.

1 Introduction

The presented work takes place in a more general framework: the modelling of unsteady mixed flows in any kind of closed pipe taking into account the cavitation problem and air entrapment. We are interested in flows occurring in closed pipes with non uniform sections, where some parts of the flow can

*email: Christian.Bourdarias@univ-savoie.fr,
†email: Mehmet.Ersoy@univ-savoie.fr,
‡email: Stephane.Gerbi@univ-savoie.fr

be free surface (it means that only a part of the pipe is filled) and other parts are pressurized (it means that the pipe is full). The transition phenomenon between the two types of flows occurs in many situations such as storm sewers, waste or supply pipes in hydroelectric installations. It can be induced by sudden changes in the boundary conditions as failure pumping. During this process, the pressure can reach severe values and may cause damages. The simulation of such a phenomenon is thus a major challenge and a great amount of works was devoted to it these last years (see [13],[14],[25],[29], for instance).

The classical shallow water equations are commonly used to describe free surface flows in open channels. They are also used in the study of mixed flows using the Preissman slot artefact (see for example [13, 29]). However, this technic does not take into account the depressurisation phenomenon which occurs during a water hammer except in recent works [21, 20, 22]. On the other hand the Allievi equations, commonly used to describe pressurized flows, are written in a non-conservative form which is not well adapted to a natural coupling with the shallow water equations.

A model for the unsteady mixed water flows in closed pipes and a finite volume discretisation have been previously studied by two of the authors [7] and a kinetic formulation has been proposed in [9]. We propose here the **PFS**-model which tends to extend naturally the work in [7] in the case of a closed pipe with non uniform section. For the sake of simplicity, we do not deal with the deformation of the domain induced by the change of pressure. We will consider only an infinitely rigid pipe.

The paper is organized as follows. Section 2 is devoted to the derivation of the free surface model from the 3D *incompressible* Euler equations which are written in a suitable local reference frame (following [3, 4]) in order to take into account the local effects produced by the changes of section and the slope variation. The construction of the free surface model is done by a formal asymptotic analysis. Seeking for an approximation at first order gives the model called **FS**-model. In Section 3, we adapt the derivation of the **FS**-model to derive the pressurized model, called **P**-model, from the 3D *compressible* Euler equations. Writing the source terms of these two models, **P** and **FS**-model, into a unified form and using the same couple of conservative unknowns as in [8], we propose in Section 4 a model for mixed flows, that we call **PFS**-model . We state some mathematical properties of this model. Section 5 is devoted to the extension of the VFRoe scheme described in [12, 16, 7] that was used for the case of uniform pipes. In Section 6, we show how to construct a convection matrix in order to get an exactly well-balanced scheme. Several numerical tests are presented in Section 7.

Notations concerning geometrical variables

- $(0, \mathbf{i}, \mathbf{j}, \mathbf{k})$: cartesian reference frame
- $\omega(x, 0, b(x))$: parametrization in the reference frame $(0, \mathbf{i}, \mathbf{j}, \mathbf{k})$ of the plane curve $\mathcal{C}$ which corresponds to the main flow axis
- $(\mathbf{T}, \mathbf{N}, \mathbf{B})$: Serret-Frenet reference frame attached to $\mathcal{C}$ with $\mathbf{T}$ the tangent vector, $\mathbf{N}$ the normal vector and $\mathbf{B}$ the binormal vector
- X, Y, Z: local variable in the Serret Frenet reference frame with X the curvilinear abscissa, Y the width of pipe, Z the $\mathbf{B}$-coordinate of any particle.
- $\sigma(X, Z) = \beta(X, Z) - \alpha(X, Z)$: width of the pipe at altitude Z with $\beta(X, Z)$ (resp. $\alpha(X, Z)$) is the Y-coordinate of right (resp. left) boundary point at altitude Z
- $\theta(X)$: angle $(\mathbf{i}, \mathbf{T})$
- $S(X)$: cross-section area
- $R(X)$: radius of the cross-section $S(X)$
- $\mathbf{n_{wb}}$: outward normal vector to the wet part of the pipe
- $\mathbf{n}$: outward normal vector at the boundary point m in the Ω-plane defined below

Notations concerning the free surface (FS) part

- A: wet area
- Q: discharge
- $\Omega(t, X)$: free surface cross section
- $H(t, X)$: physical water height
- $h(t, X)$: Z-coordinate of the water level, $\sigma(X, h(t, X)) = T(A)$: width of the free surface
- $\mathbf{n_{fs}}$: outward $\mathbf{B}$-normal vector to the free surface
- ρ_0: density of the water at atmospheric pressure p_0

Notations concerning the pressurized part

- $\Omega(X)$: pressurized cross section
- $\rho(t, X)$: density of the water
- β: water compressibility coefficient
- $c = \frac{1}{\sqrt{\beta\, \rho_0}}$: sonic speed
- $A = \frac{\rho}{\rho_0} S$: FS equivalent wet area
- Q: FS equivalent discharge

Notations concerning the PFS model

- $\mathbf{S}$: the physical wet area: $\mathbf{S} = A$ if the state is free surface, S otherwise
- $\mathcal{H}$: the Z coordinate of the water level: $\mathcal{H} = h$ if the state is free surface, R otherwise

Other notations

- Bold characters are used for vectors except for $\mathbf{S}$

2 Formal derivation of the FS-model for free surface flows

The classical shallow water equations are used to describe physical situations like rivers, coastal domains, oceans and sedimentation problems. These equations are obtained from the incompressible Euler system (see e.g. [2, 23]) or from the incompressible Navier-Stokes system (see for instance [10, 11, 17, 24]) by several techniques (e.g. by direct integration or asymptotic analysis). We adapt here the derivation in [3, 4] to get a new unidirectional shallow water model. We start from the 3D incompressible Euler equations where we neglect the acceleration following the y-axis supposing the existence of a privileged main flow axis. We write then the Euler equations in the local Serret-Frenet reference frame in order to take into account the local effects produced by the changes of section and the slope variation. Then we derive a shallow water model by a formal asymptotic analysis (done in Subsection 2.3).

2.1 Incompressible Euler equations and framework

Let us consider the cartesian reference frame $(O, \mathbf{i}, \mathbf{j}, \mathbf{k})$. In the corresponding coordinate system (x, y, z), the 3D incompressible Euler system writes:

$$\left\{ \begin{array}{rcl} \operatorname{div}(\rho_0 \, \mathbf{U}) & = & 0 \\ \partial_t(\rho_0 \, \mathbf{U}) + \rho_0 \, \mathbf{U} \cdot \nabla(\rho_0 \, \mathbf{U}) + \nabla P & = & \mathbf{F} \end{array} \right. \tag{1}$$

where $\mathbf{U}(t, x, y, z)$ denotes the velocity with components (u, v, w), $P = p(t, x, y, z) I_3$ is the isotropic pressure tensor, ρ_0 the density of the fluid at atmospheric pressure p_0 and $\mathbf{F}$ is the exterior strength of gravity.
We close classically System (1) using a kinematic law for the evolution of the free surface: *any free surface particle is advected by the fluid velocity* $\mathbf{U}$ and on the wet boundary, we assume the no-leak condition $\mathbf{U}.\mathbf{n_{wb}} = 0$ where $\mathbf{n_{wb}}$ is the outward unit normal vector to the wet part of the pipe (see Fig. 2). We set the pressure P to 0 at the free surface.
We define the domain $\Omega_F(t)$ of the flow at time t as the union of sections $\Omega(t, x)$ (assumed to be simply connected compact sets) orthogonal to some plane curve $\mathcal{C}$ lying in $(O, \mathbf{i}, \mathbf{k})$ to follow the privileged main flow axis. We choose the parametrization $(x, 0, b(x))$ in the cartesian reference frame $(O, \mathbf{i}, \mathbf{j}, \mathbf{k})$ where $\mathbf{k}$ follows the vertical direction; $b(x)$ is then the elevation of the point $\omega(x, 0, b(x))$ over the plane $(O, \mathbf{i}, \mathbf{j})$ (see Fig. 1).
We define a local reference frame as follows: we introduce the curvilinear variable defined by:

$$X = \int_{x_0}^{x} \sqrt{1 + (b'(\xi))^2} d\xi$$

where x_0 is an arbitrary abscissa. We set $Y = y$ and we denote by Z the $\mathbf{B}$-coordinate of any fluid particle M in the Serret-Frenet reference frame $(\mathbf{T}, \mathbf{N}, \mathbf{B})$

at point $\omega(x, 0, b(x))$ with $\mathbf{T}$ the tangent vector $\mathbf{N}$, the normal and $\mathbf{B}$ the binormal vector (see FIG. 1 and FIG. 3 for the notations). $\mathbf{B}$ is normal to $\mathcal{C}$ in the vertical plane $(O, \mathbf{i}, \mathbf{k})$.
Then, at each point ω, $\Omega(t, X)$ is defined by the set:

$$\left\{(y, Z) \in \mathbb{R}^2; Z \in [-R(X), -R(X) + H(t, X)],\, y \in [\alpha(X, Z), \beta(X, Z)]\right\}$$

where $R(X)$ denotes the radius, $H(t, X)$ the physical water height at section $\Omega(t, X)$. We denote $\alpha(X, Z)$ (respectively $\beta(X, Z)$) Y-coordinate of the left (respectively right) boundary point of the domain at altitude Z, $-R(X) < Z < R(X)$ (see FIG. 3). We denote also $-R(X) + H(t, X)$ by $h(t, X)$ which is the Z-coordinate of the water level.

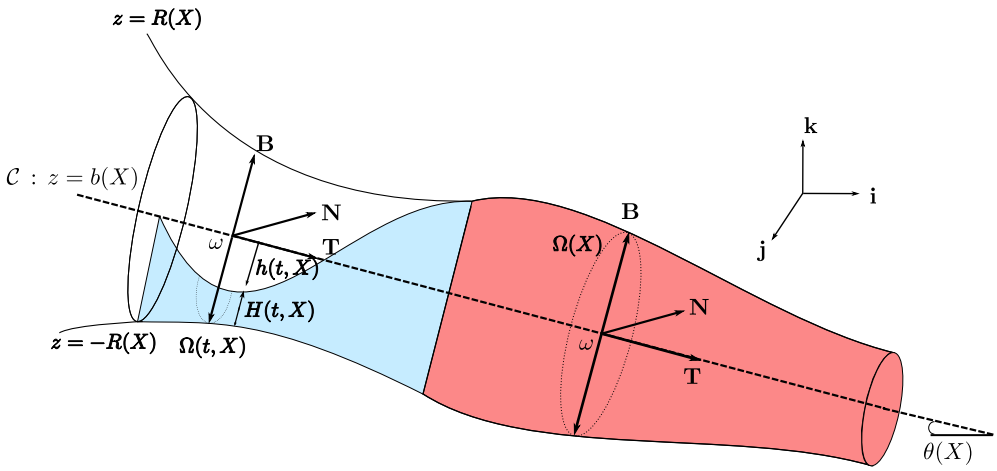

Figure 1: Geometric characteristics of the domain
Mixed flow: free surface and pressurized

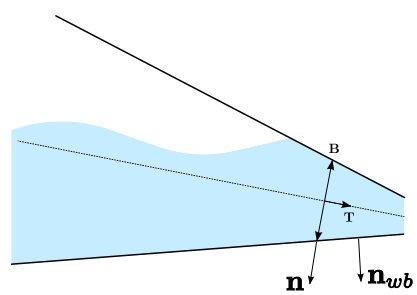

Figure 2: Outward unit normal $\mathbf{n_{wb}} \neq \mathbf{n}$ (except for uniform pipes)

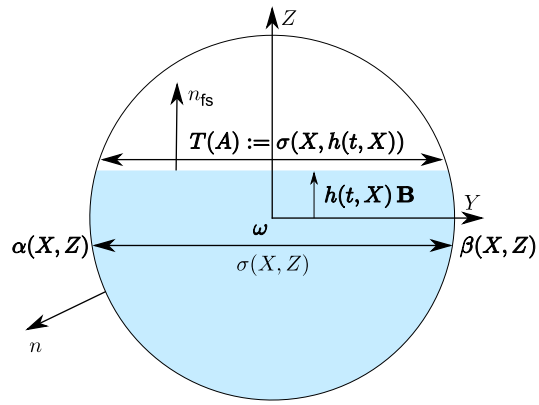

Figure 3: Cross-section $\Omega(t, X)$ of the domain at point ω in the free surface case

In the sequel, we will use a curvilinear map which will be an admissible transformation under the geometrical hypothesis on the domain:

(H) Let $\mathcal{R}(x)$ be the algebraic curvature radius of the plane curve $x \mapsto (x, 0, b(x))$. We assume that:

$$\forall x \in \Omega_F,\ |\mathcal{R}(x)| > R(x).$$

2.2 Incompressible Euler model in the curvilinear coordinates

Following the work in [3, 4], we write System (1) in the Serret-Frenet reference frame $(\mathbf{T}, \mathbf{N}, \mathbf{B})$ at point $\omega(x, 0, b(x))$ by the transformation $\mathcal{T} : (x, y, z) \to (X, Y, Z)$ using the divergence chain rule lemma that we recall here:

Lemma 2.1 *Let $(X, Y, Z) \mapsto \mathcal{T}(X, Y, Z) = (x, y, z)$ be a C^1 diffeomorphism and*
$\mathcal{A}^{-1} = \nabla_{(X,Y,Z)}\mathcal{T}$ the jacobian matrix of the transformation with determinant J.
Then, for any vector field Φ, one has:

$$J\mathrm{div}_{(x,y,z)}\Phi = \mathrm{div}_{(X,Y,Z)}(J\mathcal{A}\Phi)\,,$$

and, for any scalar function f, one has:

$$\nabla_{(x,y,z)}f = \mathcal{A}^t\nabla_{(X,Y,Z)}f,$$

where $\mathcal{A}^t$ stands for the transpose of the matrix $\mathcal{A}$.

Let $(U, V, W)^t$ be the components of the velocity vector in the (X, Y, Z) coordinates defined as $(U, V, W)^t = \Theta(u, v, w)^t$ where Θ is the matrix

$$\Theta = \begin{pmatrix} \cos\theta & 0 & \sin\theta \\ 0 & 1 & 0 \\ -\sin\theta & 0 & \cos\theta \end{pmatrix}\,,$$

where we denote by $\theta(x)$ the angle $(\mathbf{i}, \mathbf{T})$ in the $(\mathbf{i}, \mathbf{k})$ plane.
Using Lemma 2.1, the incompressible Euler system in the variables (X, Y, Z) reads:

$$\left\{\begin{array}{lcl} \partial_X(\rho_0 U) + \partial_Y(J\rho_0 V) + \partial_Z(J\rho_0 W) & = & 0 \\ \partial_t(J\rho_0 U) + \partial_X(\rho_0 U^2) + \partial_Y(J\rho_0 UV) + \partial_Z(J\rho_0 UW) + \partial_X p & = & G_1 \\ \partial_t(J\rho_0 V) + \partial_X(\rho_0 UV) + \partial_Y(J\rho_0 V^2) + \partial_Z(J\rho_0 VW) + \partial_Y(Jp) & = & 0 \\ \partial_t(J\rho_0 W) + \partial_X(\rho_0 UW) + \partial_Y(J\rho_0 VW) + \partial_Z(J\rho_0 W^2) + J\partial_Z(p) & = & G_2 \end{array}\right. \tag{2}$$

where $J(X, Y, Z) = 1 - Z\theta'(X)$ is the determinant of the transformation and

$$G_1 = \rho_0 UW\theta'(X) - Jg\rho_0 \sin\theta,\ G_2 = -\rho_0 U^2\theta'(X) - Jg\rho_0 \cos\theta.$$

The interested reader can find the details of the calculus in [3]. We have denoted by f' the derivative with respect to the space variable X of any function $f(X)$.
On the wet boundary, the no-leak condition reads:

$$(U, V, W)^t.\mathbf{n_{wb}} = 0\,. \tag{3}$$

Remark 2.1 *Notice that $\kappa(X) = \theta'(X)$ is the algebraic curvature of the axis at point $\omega(X, 0, b(X))$ and the function $J(X, Y, Z) = 1 - Z\kappa(X)$ depends only on the variables X, Z. Moreover, under the hypothesis (H), we have $J > 0$ in Ω_F. Consequently, $\mathcal{T}$ defines a diffeomorphism and thus the performed transformation is admissible.*

2.3 Formal derivation of the FS-model for free surface flows

In this section, we perform a formal asymptotic analysis on System (2). According to the work in [3, 17, 24], the shallow water equations can be obtained from the incompressible Navier-Stokes equations with particular boundary conditions. Here, we perform this analysis directly on the incompressible Euler system in order to get $J = 1 + O(\epsilon)$ for some small parameter ϵ.
Let us introduce the usual small parameter $\epsilon = H/L$ where H (the height) and L (the length) are two characteristics dimensions along the $\mathbf{B}$ and $\mathbf{T}$ axis respectively. Moreover, we assume that the characteristic dimension along the $\mathbf{j}$ axis is the same as for the $\mathbf{k}$ axis. We introduce the other characteristics dimensions $T, P, \overline{U}, \overline{V}, \overline{W}$ for time, pressure and velocity respectively and the dimensionless quantities as follows:

$$\widetilde{U} = U/\overline{U},\ \widetilde{V} = \epsilon V/\overline{U},\ \widetilde{W} = \epsilon W/\overline{U},$$

$$\widetilde{X} = X/L,\ \widetilde{Y} = Y/H,\ \widetilde{Z} = Z/H,\ \widetilde{p} = p/P, \widetilde{\theta} = \theta, \widetilde{\rho} = \rho_0.$$

In the sequel, we set $P = \overline{U}^2$ and $L = T\overline{U}$ (i.e. we only consider laminar flows).

Under these hypotheses, we have $\widetilde{J}(\widetilde{X},\widetilde{Y},\widetilde{Z}) = 1-\epsilon\widetilde{Z}\widetilde{\theta}'(\widetilde{X})$. Thus, the rescaled System (2) reads:

$$\left\{\begin{array}{rcl} \partial_{\widetilde{X}}\widetilde{U} + \partial_{\widetilde{Y}}(\widetilde{J}\widetilde{V}) + \partial_{\widetilde{Z}}(\widetilde{J}\widetilde{W}) & = & 0 \\ \partial_{\widetilde{t}}(\widetilde{J}\widetilde{U}) + \partial_{\widetilde{X}}(\widetilde{U}^2) + \partial_{\widetilde{Y}}(\widetilde{J}\widetilde{U}\widetilde{V}) + \partial_{\widetilde{Z}}(\widetilde{J}\widetilde{U}\widetilde{W}) + \partial_{\widetilde{X}}\widetilde{p} & = & G_1 \\ \epsilon^2\left(\partial_{\widetilde{t}}(\widetilde{J}\widetilde{V}) + \partial_{\widetilde{X}}(\widetilde{U}\widetilde{V}) + \partial_{\widetilde{Y}}(\widetilde{J}\widetilde{V}^2) + \partial_{\widetilde{Z}}(\widetilde{J}\widetilde{V}\widetilde{W})\right) + \partial_{\widetilde{Y}}(\widetilde{J}\widetilde{p}) & = & 0 \\ \epsilon^2\left(\partial_{\widetilde{t}}(\widetilde{J}\widetilde{W}) + \partial_{\widetilde{X}}(\widetilde{U}\widetilde{W}) + \partial_{\widetilde{Y}}(\widetilde{J}\widetilde{V}\widetilde{W}) + \partial_{\widetilde{Z}}(\widetilde{J}\widetilde{W}^2)\right) & & \\ +\widetilde{J}\partial_{\widetilde{Z}}(\widetilde{p}) = G_2 & & \end{array}\right. \quad (4)$$

where

$$G_1 = \epsilon\widetilde{U}\widetilde{W}\widetilde{\kappa}(\widetilde{X}) - \frac{\sin\widetilde{\theta}}{{F_{r,L}}^2} - \frac{\widetilde{Z}}{{F_{r,H}}^2}(\cos\widetilde{\theta})',$$

$$G_2 = -\epsilon\widetilde{U}^2\widetilde{\rho}(\widetilde{X}) - \frac{\cos\widetilde{\theta}}{{F_{r,H}}^2} + \epsilon\kappa(X)\frac{\widetilde{Z}\widetilde{J}\cos\widetilde{\theta}}{{F_{r,H}}^2},$$

$F_{r,M} = \dfrac{\overline{U}}{\sqrt{gM}}$ is the Froude number along the **T** axis and the **B** or **N** axis where M is any generic variable equal to L or H.
Formally, when ϵ vanishes, System (4) reduces to:

$$\partial_{\widetilde{X}}\widetilde{U} + \partial_{\widetilde{Y}}(\widetilde{V}) + \partial_{\widetilde{Z}}(\widetilde{W}) = 0 \quad (5)$$

$$\partial_{\widetilde{t}}(\widetilde{U}) + \partial_{\widetilde{X}}(\widetilde{U}^2) + \partial_{\widetilde{Y}}(\widetilde{U}\widetilde{V}) + \partial_{\widetilde{Z}}(\widetilde{U}\widetilde{W}) + \partial_{\widetilde{X}}\widetilde{p} = -\frac{\sin\widetilde{\theta}}{{F_{r,L}}^2} - \frac{\widetilde{Z}}{{F_{r,H}}^2}(\cos\widetilde{\theta})' \quad (6)$$

$$\partial_{\widetilde{Z}}(\widetilde{p}) = -\frac{\cos\widetilde{\theta}}{{F_{r,H}}^2} \quad (7)$$

Let us introduce the conservative variables $A(t,X)$ and $Q(t,X)$ representing respectively the wet area and the discharge defined as:

$$A(t,X) = \int_{\Omega(t,X)} dY dZ, \quad Q(t,X) = A(t,X)\overline{U}$$

where $\overline{U}$ is the mean value of the velocity :

$$\overline{U}(t,X) = \frac{1}{A(t,X)}\int_{\Omega(t,X)} U(t,X)\ dY dZ\,.$$

We integrate the preceding system (5-6-7) along the cross-section with the approximation $\overline{U^2} \approx \overline{U}\,\overline{U}$ and $\overline{U\,V} \approx \overline{U}\,\overline{V}$. Then, returning to the physical variables, the free surface model, that we call **FS**-model, reads:

$$\left\{\begin{array}{rcl} \partial_t A + \partial_X Q & = & 0 \\ \partial_t Q + \partial_X\left(\dfrac{Q^2}{A} + gI_1(X,A)\cos\theta\right) & = & gI_2(X,A)\cos\theta - gA\sin\theta \\ & & -gA\overline{Z}(X,A)(\cos\theta)' \end{array}\right. \quad (8)$$

where $I_1(X,A)$ and $I_2(X,A)$ are respectively the classical term of hydrostatic pressure and the pressure source term defined by:

$$I_1(X,A) = \int_{-R}^{h} (h-Z)\sigma\, dZ \text{ and } I_2(X,A) = \int_{-R}^{h} (h-Z)\partial_X \sigma\, dZ$$

which are obtained from the integration of the pressure term $\partial_{\widetilde{X}}\widetilde{p}$ in Equation (5) with $\widetilde{p} = \rho(h(t,X)-Z)\cos\theta$ (obtained from equation (7)).
In these formulas $\sigma(X,Z)$ is the width of the cross-section at position X and at height Z. The additional term $\overline{Z}(X,A)$ is defined by $(h(A) - I_1(X,A)/A)$. It is the Z-coordinate of the center of mass:

$$\begin{aligned} \overline{Z} &= \int_{\Omega(t,X)} Z\, dY\, dZ \\ &= \int_{-R(X)}^{h(t,X)} \int_{\alpha(X,Z)}^{\beta(X,Z)} Z\, dY\, dZ \\ &= \int_{-R(X)}^{h(t,X)} Z\, \sigma(X,Z)\, dZ \end{aligned} .$$

In System (8), we may add a friction term $-\rho_0 g S_f\, \mathbf{T}$ to take into account the dissipation of energy. We have chosen this term S_f as the one given by the Manning-Strickler law (see e.g. [29]):

$$S_f(A,U) = K(A)U|U|\,.$$

The term $K(A)$ is defined by: $K(A) = \dfrac{1}{K_s^2 R_h(A)^{4/3}}$, $K_s > 0$ is the Strickler coefficient of roughness depending on the material, $R_h(A) = A/P_m$ is the hydraulic radius and P_m is the perimeter of the wet surface area (length of the part of the channel's section in contact with the water).

3 Formal derivation of the P-model for pressurized flows

In this section, we present a new set of unidirectional shallow water like equations to describe pressurized flows in closed non uniform water pipes. This model is constructed to be coupled in natural way with the **FS**-model (8). Starting from the 3D compressible Euler equations in cartesian coordinates,

$$\partial_t \rho + \operatorname{div}(\rho \mathbf{U}) = 0, \tag{9}$$

$$\partial_t(\rho\mathbf{U}) + \operatorname{div}(\rho\mathbf{U}\otimes\mathbf{U}) + \nabla p = \mathbf{F}, \tag{10}$$

where $\mathbf{U}(t,x,y,z)$ and $\rho(t,x,y,z))$ denotes the velocity with components (u,v,w) and the density respectively. $p(t,x,y,z)$ is the scalar pressure and $\mathbf{F}$ the exterior strength of gravity.

We define the pressurized domain of the flow as the continuous extension of Ω_F (see Subsection 2.1) defined by some plane curve $\mathcal{C}$ with parametrization $(x, 0, b(x))$ in the cartesian reference frame $(O, \mathbf{i}, \mathbf{j}, \mathbf{k})$; we recall that $b(x)$ is then the elevation of the point ω over the plane $(O, \mathbf{i}, \mathbf{j})$ (see FIG. 1). The curve may be, for instance, the axis spanned by the center of mass of each orthogonal section $\Omega(x)$ to the main mean flow axis, particularly in the case of a piecewise cone-shaped pipe. Notice that we consider only the case of infinitely rigid pipes, thus the sections $\Omega = \Omega(x)$ are only x-dependent.
We then write Equations (9-10) in the (X, Y, Z) coordinates introduced in Subsection 2.1. As we want a unidirectional model, we suppose that the mean flow follows the X-axis. To this end, we neglect the second and third equation for the conservation of the momentum.
By a straightforward computation, the mass and the first momentum conservation equation in the (X, Y, Z) coordinates reads:

$$\left\{\begin{array}{rcl} \partial_t(J\rho) + \partial_X(\rho U) + \partial_Y(\rho JV) + \partial_Z(\rho JW) & = & 0 \\ \partial_t(J\rho U) + \partial_X(\rho U^2) + \partial_Y(\rho JUV^2) + \partial_Z(\rho JUW) + \partial_X p & & \\ = -\rho Jg\sin\theta + \rho UW(\cos\theta)' & & \end{array}\right. \tag{11}$$

Applying the same asymptotic analysis developed in Subsection 2.3, Equations (9-10) read:

$$\left\{\begin{array}{rcl} \partial_t(\rho) + \partial_X(\rho U) + \partial_Y(\rho V) + \partial_Z(\rho W) & = & 0 \\ \partial_t(\rho U) + \partial_X(\rho U^2) + \partial_Y(\rho UV) + \partial_Z(\rho UW) + \partial_X p & = & -\rho g\sin\theta \\ & & -gZ(\cos\theta)' \end{array}\right. \tag{12}$$

We choose the linearized pressure law:

$$p = p_a + \frac{\rho - \rho_0}{\beta\rho_0} \tag{13}$$

(see e.g. [29, 30]) in which ρ_0 represents the density of the fluid at atmospheric pressure p_0, p_a is some function set to zero and β the water compressibility coefficient (equal to $5.0\,10^{-10}\,m^2.N^{-1}$ in practice). The sonic speed is then given by $c = 1/\sqrt{\beta\rho_0}$ and thus $c \approx 1400\,m.s^{-1}$.
For $m \in \partial\Omega$, $\mathbf{n} = \dfrac{\mathbf{m}}{|\mathbf{m}|}$ is the outward unit vector at the point m in the Ω-plane and $\mathbf{m}$ stands for the vector ωm (as displayed on FIG. 3).
Following the section-averaging method performed in Subsection 2.3, we integrate System (12) over the cross-section Ω. Noting the averaged values over Ω by the overlined letters (except $\overline{Z}$), and using the approximations $\overline{\rho U} \approx \overline{\rho}\,\overline{U}$, $\overline{\rho U^2} \approx$

$\overline{\rho}\overline{U}^2$ the shallow water like equations read:

$$\begin{aligned}
\partial_t(\overline{\rho}S) + \partial_X(\overline{\rho}S\overline{U}) &= \int_{\partial\Omega} \rho\,(U\partial_X\mathbf{m} - \mathbf{V})\,.\mathbf{n}\,ds && (14)\\
\partial_t(\overline{\rho}S\overline{U}) + \partial_X(\overline{\rho}S\overline{U} + c^2\overline{\rho}S) &= -g\overline{\rho}S\sin\theta + c^2\overline{\rho}S' \\
&- g\overline{\rho}S\overline{Z}(\cos\theta)' && (15)\\
&+ \int_{\partial\Omega} \rho U\,(U\partial_X\mathbf{m} - \mathbf{V})\,.\mathbf{n}\,ds
\end{aligned}$$

where $\mathbf{V} = (V, W)^t$ is the velocity in the $(\mathbf{N}, \mathbf{B})$-plane. We denote by S the area of the cross-section of the pipe at position X.
The integral terms appearing in (14) and (15) vanish, as the pipe is infinitely rigid, i.e. $\Omega = \Omega(X)$ (see [8] for the dilatable case). It follows the non-penetration condition (see Fig. 4):

$$\begin{pmatrix} U \\ V \\ W \end{pmatrix}.\mathbf{n_{wb}} = 0\,.$$

Omitting the overlined letters (except $\overline{Z}$), we introduce the conservative variables

$$A = \frac{\rho}{\rho_0}S \qquad \text{the FS } \textit{equivalent wet area} \tag{16}$$

$$Q = AU \qquad \text{the FS } \textit{equivalent discharge}\,. \tag{17}$$

and dividing Equations (14)-(15) by ρ_0 we get:

$$\left\{\begin{aligned}
\partial_t(A) + \partial_X(Q) &= 0 \\
\partial_t(Q) + \partial_X\left(\frac{Q^2}{A} + c^2A\right) &= -gA\sin\theta - gA\overline{Z}(X,S)(\cos\theta)' \\
&\quad + c^2A\frac{S'}{S}
\end{aligned}\right. \tag{18}$$

As introduced previously for the **FS**-model in Section (2.3), we may introduce the friction term $-\rho g S_f\,\mathbf{T}$ given by the Manning-Strickler law (see e.g. [29]):

$$S_f(S,U) = K(S)U|U|$$

where $K(S)$ is defined by: $K(S) = \dfrac{1}{K_s^2 R_h(S)^{4/3}}$, $K_s > 0$ is the Strickler coefficient of roughness depending on the material and $R_h(S) = S/P_m$ is the hydraulic radius where P_m is the perimeter of the wet surface area (length of the part of the channel's section in contact with the water, equal to $2\,\pi\,R$ in the case of circular pipe).

This choice of variables is motivated by the fact that this system is formally close to the **FS**-model (8) where the terms $gI_1(X,A)\cos\theta$, $gI_2(X,A)\cos\theta$, $\overline{Z}(X,A)$ are respectively the counterparts of c^2A, $c^2A\dfrac{S'}{S}$, $\overline{Z}(X,S)$ in System (18). Let us remark that the term $\overline{Z}$ is continuous through the change of state (pressurized to free surface or free surface to pressurized state) when the same curve plane is chosen (in practice, the main axis of the pipe). Then, we are motivated to connect "continuously" System (8) and (18) through transition points (through the change of state) by defining a continuous pressure law. It leads to a "natural" coupling between the pressurized and free surface model as we will see in Section 4.

4 The PFS-model

The formulations of the **FS**-model (8) and **P**-model (18) are very close to each other. The main difference comes from the pressure law. In order to build a coupling between the two models, we have to define a pressure that ensures its continuity through transition points in the same spirit of [7]. As pointed out in the previous section, we will use the common couple of unknowns (A,Q) and the same plane curve $\mathcal{C}$ (see Remark 4.1) to get a continuous model for mixed flows.

Remark 4.1 *The plane curve with parametrization $(x,0,b(x))$ is chosen as the main pipe axis in the axisymmetric case. Actually this choice is the more convenient for pressurized flows while the bottom line is adapted to free surface flows. Thus we must assume small variations of the section (S' small) or equivalently small angle φ as displayed on* FIG. *4.*

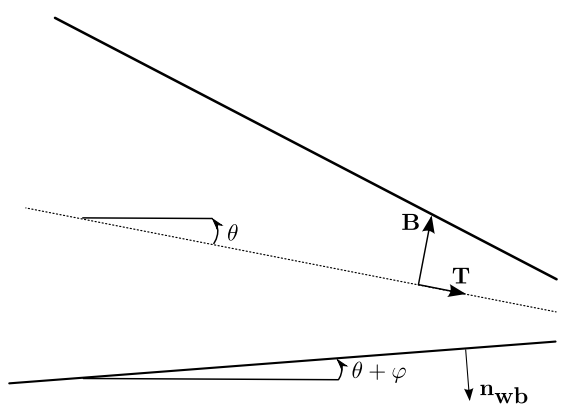

Figure 4: Some restriction concerning the geometric domain.

We introduce a state indicator E (see FIG. 4) such that:

$$E = \begin{cases} 1 & \text{if the state is pressurized: } (\rho \neq \rho_0) \\ 0 & \text{if the state is free surface: } (\rho = \rho_0) \end{cases} . \tag{19}$$

Next, we define the *physical wet area* $\mathbf{S}$ by:

$$\mathbf{S} = \mathbf{S}(A, E) = \begin{cases} S & \text{if} \quad E = 1 \\ A & \text{if} \quad E = 0 \end{cases} \tag{20}$$

and a modified pressure law (see FIG. 4) which ensures its continuity through the change of state by:

$$p(X, A, E) = c^2(A - \mathbf{S}) + gI_1(X, \mathbf{S}) \cos\theta. \tag{21}$$

Remark 4.2

- *Indeed, when a change of state occurs we have:*

$$\lim_{\substack{A \to S \\ A < S}} p(X, A, E) = \lim_{\substack{A \to S \\ A > S}} p(X, A, E) = gI_1(X, S)\cos(\theta)$$

  which ensures the continuity of the pressure.

- *The flux gradient F is discontinuous through the change of state since*

$$\frac{\partial F}{\partial A}(A, Q, 0) = g\frac{\partial}{\partial A} I_1(X, A)\cos\theta \neq c^2 = \frac{\partial F}{\partial A}(A, Q, 1).$$

Finally, from the **P**-model (18), the **FS**-model (8), the definition of E (19), the definition of $\mathbf{S}$ (20) and the pressure law (21), the **PFS**-model for unsteady mixed flows can be simply expressed into a single formulation as:

$$\begin{cases} \partial_t(A) + \partial_X(Q) &= 0 \\ \partial_t(Q) + \partial_X\left(\dfrac{Q^2}{A} + p(X, A, E)\right) &= -gAb' + Pr(X, A, E) \\ & \quad -G(X, A, E) \\ & \quad -K(X, A, E)\dfrac{Q|Q|}{A} \end{cases} \tag{22}$$

where K, Pr, and G denotes respectively the friction, the pressure source and the geometry source term defined as follows:

$$\begin{aligned} Pr(X, A, E) &= c^2\left(\frac{A}{\mathbf{S}} - 1\right) S' + gI_2(X, \mathbf{S})\cos\theta \\ & \qquad \text{with } I_2(X, \mathbf{S}) = \int_{-R(X)}^{\mathcal{H}(\mathbf{S})} (\mathcal{H}(\mathbf{S}) - Z)\, \partial_X \sigma(X, Z)\, dZ, \\ G(X, A, E) &= gA\,\overline{Z}(X, \mathbf{S})(\cos\theta)', \\ K(X, A, E) &= \frac{1}{K_s^2 R_h(\mathbf{S})^{4/3}} \end{aligned}$$

and b' stands for $\sin\theta(X)$. $\mathcal{H}$ represents the Z-coordinate of the water level:

$$\mathcal{H} = \mathcal{H}(\mathbf{S}) = \begin{cases} h(A) & \text{if} \quad E = 0 \\ R(X) & \text{if} \quad E = 1 \end{cases} . \tag{23}$$

Remark 4.3 (Both models are recovered) *Setting $\boldsymbol{S}(A, E) = A$ in System (22), we obtain obviously the free surface model (8). For all pressurized states, when $\boldsymbol{S}(A, E) = S$, the pressure law (21) reads, for instance, in the case of circular pipe:*

$$c^2(A - S) + gI_1(X, S)\cos\theta = c^2(A - S) + g\,\pi\,R^3\,\cos\theta$$

which is not exactly the pressure law of the $\boldsymbol{P}$-model (18). Indeed, the derivation of the $\boldsymbol{P}$-model is done with the linearized pressure law (13) (see Section 3) with $p_a = 0$. Thus, the property of the continuity of models (18)-(8) through a change of state is obtained if and only if p_a is chosen as $gI_1(X, S)\cos\theta$ which is the hydrostatic pressure corresponding to a full section.

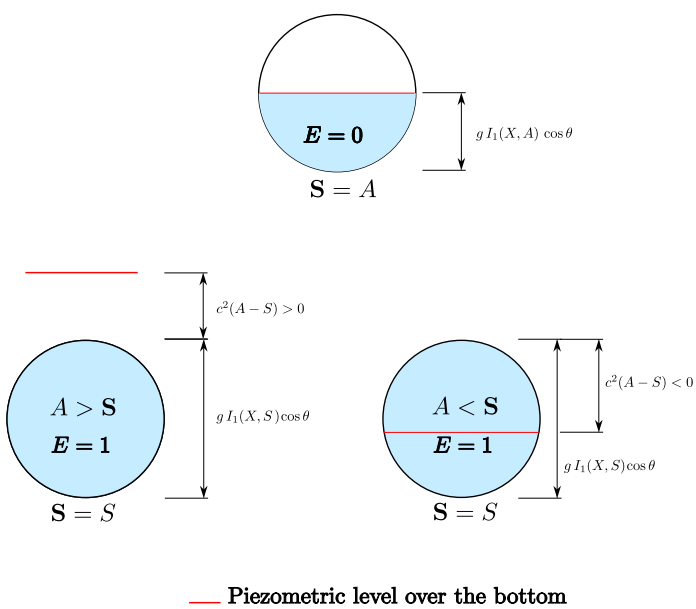

Figure 5: Free surface state $p(X, A, 0) = g\,I_1(X, A)\cos\theta$ (top), pressurized state with overpressure $p(x, A, 1) > 0$ (bottom left), pressurized state with depression $p(x, A, 1) < 0$ (bottom right).

The **PFS**-model (22) satisfies the following properties:

Theorem 4.1

1. *The right eigenvalues of System (22) are given by:*

$$\lambda^- = U - c(A,E),\ \lambda^+ = U + c(A,E)$$

with $c(A,E) = \begin{cases} \sqrt{g\,\dfrac{A}{T(A)}\cos\theta} & \text{if} \quad E=0 \\ c & \text{if} \quad E=1 \end{cases}$, *where* $T(A)$ *is the width of the free surface (see* FIG. *3).*

Then, System (22) is strictly hyperbolic on the set:

$$\{A(t,X) > 0\}\ .$$

2. *For smooth solutions, the mean velocity* $U = Q/A$ *satisfies*

$$\begin{aligned} \partial_t U + \partial_X \left(\frac{U^2}{2} + c^2 \ln(A/\boldsymbol{S}) + g\mathcal{H}(\boldsymbol{S})\cos\theta + gb \right) \\ = -gK(X,A,E)U|U| \leqslant 0. \end{aligned} \tag{24}$$

The quantity $\dfrac{U^2}{2} + c^2\ln(A/\boldsymbol{S}) + g\mathcal{H}(\boldsymbol{S})\cos\theta + gb$ *is called the total head.*

3. *The still water steady state reads:*

$$u = 0 \quad \text{and} \quad c^2\ln(A/\boldsymbol{S}) + g\mathcal{H}(\boldsymbol{S})\cos\theta + gb = 0. \tag{25}$$

4. *It admits a mathematical entropy*

$$\mathcal{E}(A,Q,E) = \frac{Q^2}{2A} + c^2 A\ln(A/\boldsymbol{S}) + c^2 S + gA\overline{Z}(X,\boldsymbol{S})\cos\theta + gAb \tag{26}$$

which satisfies the entropy relation for smooth solutions

$$\partial_t\mathcal{E} + \partial_X\Big((\mathcal{E} + p(X,A,E))\,U \Big) = -gAK(X,A,E)U^2|U| \leqslant 0\,. \tag{27}$$

Notice that the total head and $\mathcal{E}$ are defined continuously through the transition points.

Remark 4.4 *The term* $A\overline{Z}(X,A)(\cos\theta)'$ *is also called "corrective term" since it allows to write the Equations (24) and (27) with (26).*

Proof of Theorem 4.1: the results (24) and (27) are obtained in a classical way. Indeed, Equation (24) is obtained by subtracting the result of the multiplication of the mass equation by U to the momentum equation. Then

multiplying the mass equation by $\left(\frac{U^2}{2} + c^2 \ln(A/\mathbf{S}) + g\mathcal{H}(\mathbf{S})\cos\theta + gb\right)$ and adding the result of the multiplication of Equation (24) by Q, we get:

$$\begin{aligned}
&\partial_t \left(\frac{Q^2}{2A} + c^2 A \ln(A/\mathbf{S}) + c^2 S + gA\overline{Z}(X,\mathbf{S})\cos\theta + gAb\right) \\
&+\partial_X \left(\left(\frac{Q^2}{2A} + c^2 A \ln(A/\mathbf{S}) + c^2 S + gA\overline{Z}(X,\mathbf{S})\cos\theta + gAb + p(X,A,E)\right) U\right) \\
&+c^2 \left(\frac{A}{\mathbf{S}} - 1\right) \partial_t \mathbf{S} = -gAK(X,A,E)U^2|U| \leqslant 0\,.
\end{aligned}$$

We see that the term $c^2 \left(\frac{A}{\mathbf{S}} - 1\right) \partial_t \mathbf{S}$ is identically 0 since we have $\mathbf{S} = A$ when the flow is free surface whereas $\mathbf{S} = S(X)$ when the flow is pressurized. Moreover, from the last inequality, when $\mathbf{S} = A$, we have the classical entropy inequality (see [7, 8]) with $\mathcal{E}$:

$$\mathcal{E}(A,Q,E) = \frac{Q^2}{2A} + gA\overline{Z}(X,A)\cos\theta + gAb$$

while in the pressurized case, it is:

$$\mathcal{E}(A,Q,E) = \frac{Q^2}{2A} + c^2 A \ln(A/S) + c^2 S + gAb.$$

Finally, the entropy for the **PFS**-model reads:

$$\mathcal{E}(A,Q,E) = \frac{Q^2}{2A} + c^2 A \ln(A/\mathbf{S}) + c^2 S + gA\overline{Z}(X,\mathbf{S})\cos\theta + gAb.$$

Let us remark that the term $c^2 S$ makes $\mathcal{E}$ continuous through transition points and it permits also to write the entropy flux under the classical form $(\mathcal{E} + p)U$.

■

5 Finite volume discretisation

In this section, we adapt the VFRoe scheme described in [12, 16, 7]. The new terms appearing in the **PFS**-model related to the curvature and the section variation are upwinded in the same spirit of [7]. The numerical scheme is adapted to discontinuities of the flux gradient occurring in the treatment of the transitions between free surface and pressurized states.

5.1 Discretisation of the space domain

The spatial domain is a pipe of length L. The main axis of the pipe is divided in cells $m_i = [X_{i-1/2}, X_{i+\frac{1}{2}}]$, $1 \leq i \leq N$. Δt^n denotes the timestep and we set $t_{n+1} = t_n + \Delta t^n$.

The discrete unknowns are $U_i^n = \begin{pmatrix} A_i^n \\ Q_i^n \end{pmatrix}$. For the sake of simplicity, the boundary conditions are not treated (the interested reader can find this treatment in details in [7]).

5.2 Explicit first order VFRoe scheme

We propose to extend the finite volume discretisation [7] to the **PFS**-model using the upwinding of the new source terms: the curvature and section variation of the pipe. In what follows, we do not write the E dependency.
First, following Leroux *et al.* [18, 26] we use piecewise constant functions to approximate b ($b'(X) = \sin\theta(X)$) as well as the term $\cos\theta$ and the cross section area S. Adding the equations $\partial_t Z = 0$, $\partial_t \cos\theta = 0$ and $\partial_t S = 0$, the **PFS**-model can be written under a non-conservative form with the variable $\mathbf{W} = (b, \cos\theta, S, A, Q)^t$:

$$\partial_t \mathbf{W} + \partial_X \mathbf{F}(X, \mathbf{W}) + B(X, \mathbf{W})\partial_X \mathbf{W} = TS(\mathbf{W}) \tag{28}$$

where

$$\mathbf{F}(X, \mathbf{W}) = \begin{pmatrix} 0 \\ 0 \\ 0 \\ Q \\ \dfrac{Q^2}{A} + p(X, A) \end{pmatrix}, \; TS(\mathbf{W}) = \begin{pmatrix} 0 \\ 0 \\ 0 \\ 0 \\ -g\,K(X, \mathbf{S})\,\dfrac{Q|Q|}{A} \end{pmatrix}$$

and

$$B(X, \mathbf{W}) = \begin{pmatrix} 0 & 0 & 0 & 0 & 0 \\ 0 & 0 & 0 & 0 & 0 \\ 0 & 0 & 0 & 0 & 0 \\ 0 & 0 & 0 & 0 & 0 \\ gA & gA\overline{Z} & -c^2(A/\mathbf{S} - 1) - \mathcal{I}(X, \mathbf{W}) & 0 & 0 \end{pmatrix}$$

where we have written the pressure source term due to the geometry $gI_2(X, \mathbf{S})\cos(\theta)$ as $\mathcal{I}(X, \mathbf{W})S'$. For instance, for a circular cross-section pipe we have:

$$\mathcal{I}(X, \mathbf{W}) = \frac{1}{2\,\pi}\left(\frac{\mathcal{H}(\mathbf{S})\pi}{2} + \mathcal{H}(\mathbf{S})\arcsin\left(\frac{\mathcal{H}(\mathbf{S})}{R(X)}\right) + \frac{\sigma(X, \mathcal{H}(\mathbf{S}))}{2}\right).$$

Let W_i^n be an approximation of the mean value of $\mathbf{W}$ on the mesh m_i at time t_n. Since the values of $b, \cos\theta, S$ are known, integrating the above equations over $]X_{i-1/2}, X_{i+\frac{1}{2}}[\times[t_n, t_{n+1}[$, we can write a Finite Volume scheme as follows:

$$\begin{aligned} \mathbf{W}_i^{n+1} \;=\; & \mathbf{W}_i^n - \alpha_i\Big(\mathbf{F}(\mathbf{W}_{i+1/2}^*(0^-, \mathbf{W}_i^n, \mathbf{W}_{i+1}^n)) - \mathbf{F}(\mathbf{W}_{i-1/2}^*(0^+, \mathbf{W}_{i-1}^n, \mathbf{W}_i^n))\Big) \\ & + TS(\mathbf{W}_i^n) \end{aligned} \tag{29}$$

with $\alpha_i = \dfrac{\Delta t^n}{h_i}$.

$\mathbf{W}^*_{i+1/2}(\xi = x/t, \mathbf{W}_i, \mathbf{W}_{i+1})$ is the exact or an approximate solution to the Riemann problem at interface $X_{i+1/2}$ associated to the left and right states $\mathbf{W}_i$ and $\mathbf{W}_{i+1}$. Let us also remark that the term $B(X, \mathbf{W})$ does not appear explicitly in this formulation since b', $(\cos\theta)'$ and S' are null on $]X_{i-1/2}, X_{i+\frac{1}{2}}[$ but contributes to the computation of the numerical flux.

The computation of the interface quantities $\mathbf{W}^*_{i\pm1/2}(0^\pm, \mathbf{W}_i, \mathbf{W}_{i+1})$ will depend on two types of interfaces located at the point $X_{i+\frac{1}{2}}$: the first one is a non transition point, when the flow on both sides of the interface is of the same type. The second one is a transition point, when the flow changes of type through the interface. We recall the approach used in [7] and adapt it here to the new terms. According to the type of interface, we have to solve two different linearised Riemann problems.

5.2.1 The Case of a non transition point

Expanding the term $\partial_X \mathbf{F}(X, \mathbf{W})$ in the non-conservative equations (28), the quasilinear formulation of the **PFS**-model (22) reads:

$$\partial_t \mathbf{W} + D(\mathbf{W})\, \partial_X \mathbf{W} = TS(\mathbf{W}) \tag{30}$$

with D the convection matrix defined by

$$D(\mathbf{W}) = \begin{pmatrix} 0 & 0 & 0 & 0 & 0 \\ 0 & 0 & 0 & 0 & 0 \\ 0 & 0 & 0 & 0 & 0 \\ 0 & 0 & 0 & 0 & 1 \\ gA & gA\mathcal{H}(\mathbf{S}) & \Psi(\mathbf{W}) & c^2(\mathbf{W}) - u^2 & 2u \end{pmatrix} \tag{31}$$

where $\Psi(\mathbf{W}) = gS\partial_S\mathcal{H}(\mathbf{S})\cos\theta - c^2(\mathbf{W})\dfrac{A}{\mathbf{S}}$ and $u = Q/A$ denotes the speed of the water. $c(\mathbf{W})$ is then c for the pressurized flow or $\sqrt{g\dfrac{A}{T(A)}\cos\theta}$ for the free surface flow.

Remark 5.1 *Let us remark that, since $\partial_X I_1(X, A) = I_2(X, A) + \partial_A I_1(A)\partial_X A$, the pressure source term I_2 does not appear in Equation (30).*

To compute the interface quantities denoted by (AM, QM) for the left hand side and (AP, QP) for the right hand side (see Figure 6 below), we solve the following linearised Riemann problem:

$$\left\{ \begin{array}{lcl} \partial_t \mathbf{W} + \widetilde{D}\, \partial_X \mathbf{W} & = & 0 \\ \mathbf{W} & = & \left\{ \begin{array}{lll} \mathbf{W}_l = (b_l, \cos\theta_l, S_l, A_l, Q_l)^t & \text{if} & x < 0 \\ \mathbf{W}_r = (b_r, \cos\theta_r, S_r, A_r, Q_r)^t & \text{if} & x > 0 \end{array} \right. \end{array} \right. \tag{32}$$

with $(\mathbf{W}_l, \mathbf{W}_r) = (\mathbf{W}_i, \mathbf{W}_{i+1})$ and $\widetilde{D} = \widetilde{D}(\mathbf{W}_l, \mathbf{W}_r) = D(\widetilde{\mathbf{W}})$ where $\widetilde{\mathbf{W}}$ is some approximate state of the left $\mathbf{W}_l$ and the right $\mathbf{W}_r$ state.

Remark 5.2 *We will see in Section 6 that the classical approximation* $D(\widetilde{\boldsymbol{W}})$ *of the Roe matrix* $D_{Roe}(\boldsymbol{W}_l, \boldsymbol{W}_r) = \displaystyle\int_0^1 D(\boldsymbol{W}_r + (1-s)(\boldsymbol{W}_l - \boldsymbol{W}_r))\, ds$ *defined by* $\widetilde{D} = D(\widetilde{\boldsymbol{W}}) = D\left(\dfrac{\boldsymbol{W}_l + \boldsymbol{W}_r}{2}\right)$ *is not a suitable choice to preserve the still water steady state. However, we propose in Section 6 a new approximation of* $\widetilde{D}$ *which maintains it perfectly.*

We have then $W^*(0+, \mathbf{W}_l, \mathbf{W}_r) = (b_r, \cos\theta_r, S_r, AP, QP)^t$.
The eigenvalues of the matrix $\widetilde{D}$ are $\lambda_1 = 0$, $\lambda_2 = 0$, $\lambda_3 = 0$, $\lambda_4 = \widetilde{u} - c(\widetilde{\mathbf{W}})$, $\lambda_5 = \widetilde{u} + c(\widetilde{\mathbf{W}})$ and the associated right eigenvectors:

$$r_1(\widetilde{\mathbf{W}}) = \begin{pmatrix} c^2(\widetilde{\mathbf{W}}) - \widetilde{u}^2 \\ 0 \\ 0 \\ -g\widetilde{A} \\ 0 \end{pmatrix}, \quad r_2(\widetilde{\mathbf{W}}) = \begin{pmatrix} \Psi(\widetilde{\mathbf{W}}) \\ 0 \\ -g\widetilde{A} \\ 0 \\ 0 \end{pmatrix}, \quad r_3(\widetilde{\mathbf{W}}) = \begin{pmatrix} \mathcal{H}(\widetilde{S}) \\ -1 \\ 0 \\ 0 \\ 0 \end{pmatrix},$$

$$r_4(\widetilde{\mathbf{W}}) = \begin{pmatrix} 0 \\ 0 \\ 0 \\ 1 \\ \widetilde{u} - c(\widetilde{\mathbf{W}}) \end{pmatrix}, \quad r_5(\widetilde{\mathbf{W}}) = \begin{pmatrix} 0 \\ 0 \\ 0 \\ 1 \\ \widetilde{u} + c(\widetilde{\mathbf{W}}) \end{pmatrix}.$$

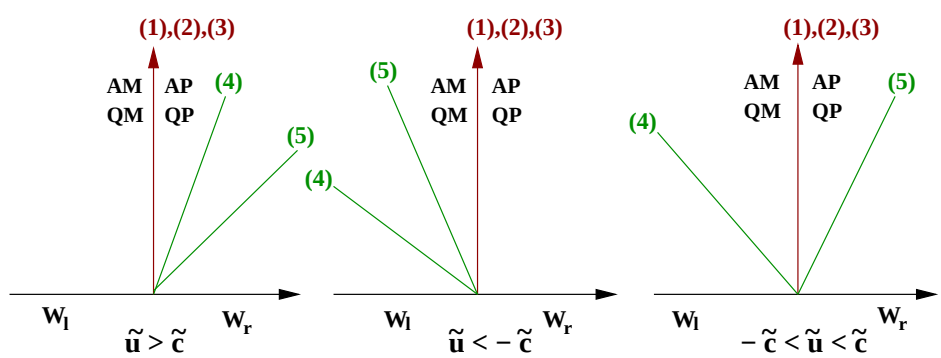

Figure 6: Solution of the Riemann problem (32). The lines (i) corresponds to the characteristic lines $X/t = \lambda_i$, for $i = 1, \ldots, 5$.

We denote P the transition matrix associated to the right eigenvectors of $\widetilde{D}$ and P^{-1} its inverse. Setting $[[\mathbf{W}]] = \mathbf{W}_r - \mathbf{W}_l$, the solution of the Riemann problem are constant states connected by shocks propagating along the characteristic lines $X/t = \lambda_i$. The jump associated to the eigenvectors r_i is then equal to $(P^{-1}\,[[\mathbf{W}]])_i\, r_i$. In particular, the discharge is continuous through the line $X/t = 0$ since the fifth component of vectors r_1, r_2 and r_3 are null. It follows that the equation associated to the wet area A remains conservative.

Thus, for instance in the subcritical case (when $-c(\widetilde{\mathbf{W}}) < \widetilde{u} < c(\widetilde{\mathbf{W}})$), we have:

$$AM = A_l + \frac{g\,\widetilde{A}}{2\,c(\widetilde{\mathbf{W}})\,(c(\widetilde{\mathbf{W}}) - \widetilde{u})}\,\psi_l^r + \frac{\widetilde{u} + c(\widetilde{\mathbf{W}})}{2\,c(\widetilde{\mathbf{W}})}\,(A_r - A_l) - \frac{1}{2\,c(\widetilde{\mathbf{W}})}\,(Q_r - Q_l)$$

$$QM = QP = Q_l - \frac{g\,\widetilde{A}}{2\,c(\widetilde{\mathbf{W}})}\,\psi_l^r + \frac{\widetilde{u}^2 - c(\widetilde{\mathbf{W}})^2}{2\,c(\widetilde{\mathbf{W}})}\,(A_r - A_l) - \frac{\widetilde{u} - c(\widetilde{\mathbf{W}})}{2\,c(\widetilde{\mathbf{W}})}\,(Q_r - Q_l)$$

$$AP = AM + \frac{g\,\widetilde{A}}{\widetilde{u}^2 - c(\widetilde{\mathbf{W}})^2}\,\psi_l^r$$

where ψ_l^r is the upwinded source term $b_r - b_l + \mathcal{H}(\widetilde{\mathbf{S}})(\cos\theta_r - \cos\theta_l) + \Psi(\widetilde{\mathbf{W}})(S_r - S_l)$.

Remark 5.3 *The friction term can also be upwinded in the same way. Writing the friction term under a conservative form*

$$\partial_X \int_{X_0}^{X} K(s, \boldsymbol{S})\,\frac{Q(t,s)|Q(t,s)|}{A^2(t,s)}\,ds$$

(for some arbitrary X_0) allows us to write the "static" slope b as a "dynamic" one as follows:

$$b + \int_{X} K(s, \boldsymbol{S})\,\frac{Q(t,s)|Q(t,s)|}{A^2(t,s)}\,ds$$

that we denote again b. Thus, the upwinding of the dynamic slope $b_{i+1} - b_i$ reads:

$$b_{i+1} - b_i + \int_{X_i}^{X_{i+1/2}} \frac{1}{K_s^2}\left\{\frac{Q|Q|}{A^2 R_h(\boldsymbol{S})^{4/3}}\right\} ds + \int_{X_{i+1/2}}^{X_{i+1}} \frac{1}{K_s^2}\left\{\frac{Q|Q|}{A^2 R_h(\boldsymbol{S})^{4/3}}\right\} ds$$

which is equal to:

$$b_{i+1} - b_i + (X_{i+1/2} - X_i)\frac{Q_i|Q_i|}{K_s^2\,A_i^2 R_h(\boldsymbol{S}_i)^{4/3}} + (X_{i+1} - X_{i+1/2})\frac{Q_{i+1}|Q_{i+1}|}{K_s^2\,A_{i+1}^2 R_h(\boldsymbol{S}_{i+1})^{4/3}}$$

since A and Q are constant on each cells.
The terminology "dynamic" and "static" slope is used since one is (t,x)-dependent while the other is only x-dependent.

5.2.2 Case of transition point

In the case of a transition point, we assume that the propagation of the interface (pressurized-free surface or free surface-pressurized) has a constant speed w during a time step. The half line $x = w\,t$ is then the discontinuity line of $\widetilde{D}(W_l, W_r)$.
Let us now consider $\mathbf{U}^- = (A^-, Q^-)$ and $\mathbf{U}^+ = (A^+, Q^+)$ the (unknown) states

respectively on the left and on the right hand side of the line $x = w\,t$ with $w = \dfrac{Q^+ - Q^-}{A^+ - A^-}$. Both states $\mathbf{U}_l$ and $\mathbf{U}^-$ (resp. $\mathbf{U}_r$ and $\mathbf{U}^+$) correspond to the same type of flow. Thus it makes sense to define the averaged matrices in each zone as follows:

- for $x < w\,t$, we set $\widetilde{D}_l = \widetilde{D}(\mathbf{W}_l, \mathbf{W}_r) = D(\widetilde{\mathbf{W}}_l)$ for some approximation $\widetilde{\mathbf{W}}_l$ which connects the state $\mathbf{W}_l$ and $\mathbf{W}^-$ (see Remark 5.2).
- for $x > w\,t$, we set $\widetilde{D}_r = \widetilde{D}(\mathbf{W}_l, \mathbf{W}_r) = D(\widetilde{\mathbf{W}}_r)$ for some approximation $\widetilde{\mathbf{W}}_l$ which connects the state $\mathbf{W}^+$ and $\mathbf{W}_r$ (see Remark 5.2).

Then we formally solve two Riemann problems and use the Rankine-Hugoniot jump conditions through the line $x = w\,t$ which writes:

$$Q^+ - Q^- = w\,(A^+ - A^-) \tag{33}$$

$$F_5(A^+, Q^+) - F_5(A^-, Q^-) = w\,(Q^+ - Q^-) \tag{34}$$

with $F_5(A, Q) = \dfrac{Q^2}{A} + p(X, A)$. According to the left ($\mathbf{U}^-$, $\mathbf{UM}$) and right unknowns ($\mathbf{U}^+$, $\mathbf{UP}$) at the interface $x_{i+1/2}$ and the sign of the speed w, we have to deal with four cases:

- pressure state propagating downstream,
- pressure state propagating upstream,
- free surface state propagating downstream,
- free surface state propagating upstream.

We can next consider two couples of "twin cases" : pressure state is propagating downstream (or upstream) as shown in the figure 7 and free surface state propagating downstream (or upstream) as shown in the figure 8. Moreover, for all existing transition case, the upwinded altitude term $b_r - b_l$ in [7] are replaced by ψ_l^r.

Pressure state propagating downstream: it is the case when on the left hand side of the line $\xi = wt$, we have a pressurized flow and on the right hand side we have a free surface flow: the speed w of the transition point being positive. Following Song [28] (see also [15]), an equivalent stationary hydraulic jump must occur from a supercritical to a subcritical condition and thus the characteristics speed satisfies the inequalities:

$$\widetilde{u}_r + c(\widetilde{\mathbf{W}})_r < w < \widetilde{u}_l + c$$

where c is the sound speed for the pressure flow, $\widetilde{u}_l$, $\widetilde{u}_r$, and $c(\widetilde{\mathbf{W}})_r$ are defined by the same formula obtained in the case of a non transition point but according to $\widetilde{D}_l$ and $\widetilde{D}_r$.

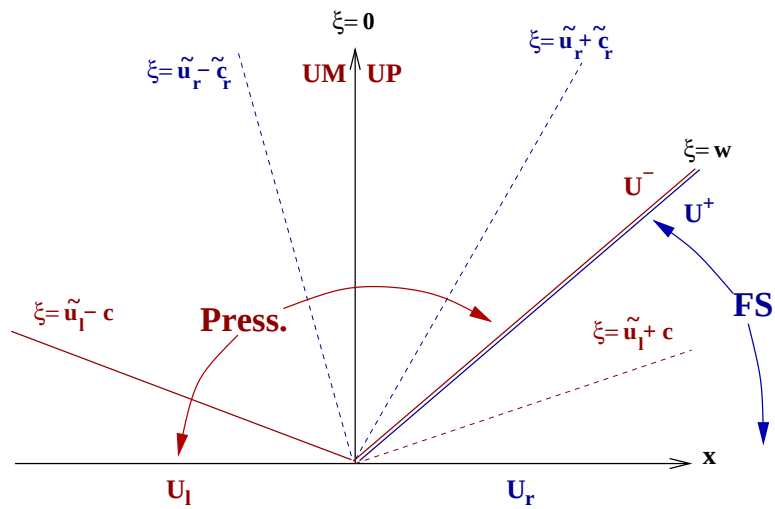

Figure 7: Pressure state propagating downstream.

Therefore, only the characteristic lines drawn with solid lines are taken into account. Indeed they are related to incoming waves with respect to the corresponding space-time area $-\infty < \xi < w$. Conversely, the dotted line $\xi = \widetilde{u}_r - c(\widetilde{\mathbf{W}})_r$, for instance, related to the free surface zone but drawn in the area of pressurized flow is a "ghost wave" and is not considered. Thus $\mathbf{U}^+ = \mathbf{U}_r$ and $\mathbf{U}_l$, $\mathbf{U}^-$ are connected through the jumps across the characteristics $\xi = 0$ and $\xi = \widetilde{u}_l - c$. Eliminating w in the Rankine-Hugoniot jump relations (33)-(34), we get $\mathbf{U}^-$ as the solution to the nonlinear system:

$$(F_5(A_r, Q_r) - F_5(A^-, Q^-)) = \frac{(Q_r - Q^-)^2}{(A_r - A^-)} \tag{35}$$

$$Q^- - Q_l - (A^- - A_l)(\widetilde{u}_l - c) + \frac{g\psi_l^r\,\widetilde{A}_l}{c + \widetilde{u}_l} \quad = \quad 0 \tag{36}$$

Finally, we obtain :

$$\begin{cases} AP & = & A^- \\ QM & = & Q^- \\ QP & = & Q^- \\ AM & = & AP - \dfrac{g\,\widetilde{A}_l\,\psi_l^r}{\widetilde{u}_l^2 - c^2}. \end{cases}$$

Free surface state propagating downstream: on the left hand side of the line $\xi = wt$ we have a free surface flow while on the right hand side, we have a pressurized flow (the speed w of the transition point being positive). Following Song [28] again, the characteristic speed satisfies the inequalities:

$$\widetilde{u}_l + c(\widetilde{\mathbf{W}})_l < w < \widetilde{u}_r + c$$

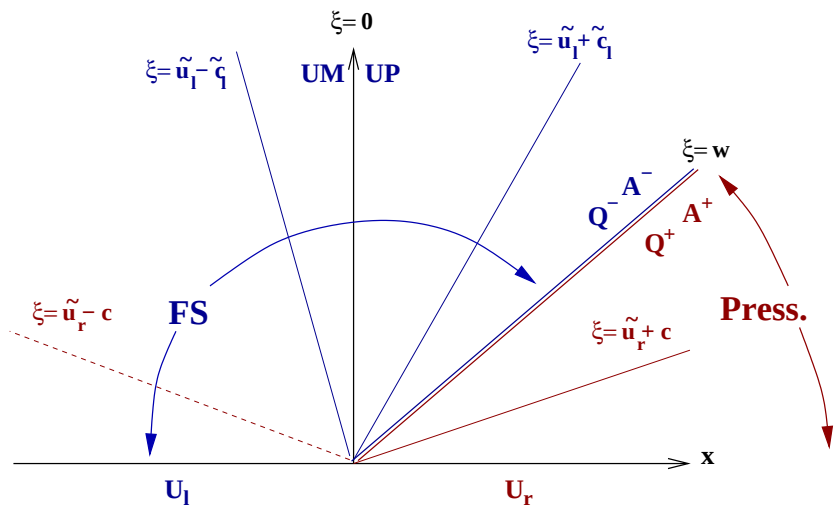

Figure 8: Free surface state propagating downstream

There are two incoming characteristic lines with respect to the free surface area $-\infty < \xi < w$ (actually three with $\xi = 0$) and they can connect the given left state $\mathbf{U}_l$ with any arbitrary free surface state **UM**. Thus only one characteristic line ($\xi = \widetilde{u}_r + c$) gives any information (it is the equation (37) above) as an incoming characteristic line with respect to the pressurized zone $w < \xi < +\infty$. From the jump relations through the characteristic $\xi = 0$, and after the elimination of w in the Rankine-Hugoniot jump relations (33),(34) we get another equation, namely Equation (38) above. It remains to close the system of four unknowns (A^-, Q^-, A^+, Q^+). Firstly, we use a jump relation across the transition point (with speed w) for the total head $\Psi = \dfrac{u^2}{2} + c^2 \ln\left(\dfrac{A}{\mathbf{S}}\right) + g\,\mathcal{H}(A)\cos\theta + g\,b$, from Equation (24), which writes:

$$\Psi^+ - \Psi^- = w\,(u^+ - u^-)\,.$$

Finally, we use the relation:

$$w = w_{pred} \;\text{ with } w_{pred} = \frac{Q_r - Q_l}{A_r - A_l}\,.$$

We have then to solve the nonlinear system:

$$(Q_r - Q^+) = (A_r - A^+)\,(\widetilde{u}_r + c) \quad (37)$$

$$(Q^+ - Q^-)\,(Q_r - Q_l) = (A_r - A_l)\,(F_2(A^+, Q^+) - F_2(A^-, Q^-)) \quad (38)$$

$$\frac{(Q^+)^2}{2\,(A^+)^2} + c^2 \ln\left(A^+\right) + g\cos\theta\,\mathcal{H}(A^+) - \frac{(Q^-)^2}{2\,(A^-)^2} - c^2 \ln\left(A^-\right) - g\cos\theta\,\mathcal{H}(A^-) = \frac{Q_r - Q_l}{A_r - A_l}\left(\frac{Q^+}{A^+} - \frac{Q^-}{A^-}\right) \quad (39)$$

$$(Q_r - Q_l)\,(A^+ - A^-) = (Q^+ - Q^-)\,(A_r - A_l) \quad (40)$$

The states **UM** et **UP** are then obtained by the following identities:

$$AM = A_l + \frac{g\,\widetilde{A}_l\,\psi_l^r}{2\,c(\widetilde{\mathbf{W}})_l(c(\widetilde{\mathbf{W}})_l - \widetilde{u}_l)} + \frac{\widetilde{u}_l + c(\widetilde{\mathbf{W}})_l}{2\,c(\widetilde{\mathbf{W}})_l}\,(A^- - A_l) - \frac{1}{2\,c(\widetilde{\mathbf{W}})_l}\,(Q^- - Q_l)$$

$$AP = AM + \frac{g\,\widetilde{A}_l\,\psi_l^r}{\widetilde{u}_l^2 - c(\widetilde{\mathbf{W}})_l^2}$$

$$QM = QP = QMP = Q_l + \frac{g\,\widetilde{A}_l\,\psi_l^r}{2\,c(\widetilde{\mathbf{W}})_l} + \frac{\widetilde{u}_l^2 - c(\widetilde{\mathbf{W}})_l^2}{2\,c(\widetilde{\mathbf{W}})_l}\,(A^- - A_l) - \frac{\widetilde{u}_l - c(\widetilde{\mathbf{W}})_l}{2\,c(\widetilde{\mathbf{W}})_l}\,(Q^- - Q_l)$$

Finally, the update state A_i^{n+1}, Q_i^{n+1} are obtained by the same relation as in the case of a non transition point.
Using equations (29) we update the values of A_i^{n+1}, Q_i^{n+1} with a standard stability condition of Courant-Friedrich-Levy controlling the time step size Δt^n.

5.2.3 Updating the state of the flow E in a cell.

To update the state E in the cell m_i (see Fig. 9), we use a discrete version of the state indicator E defined by (19) equal to 1 for a pressurized flow and 0 otherwise. Following [7], after the computation of the wet area A_i^{n+1} we predict the state of the flow in the cell m_i by the following criterion:

- if $E_i^n = 0$ then :
  if $A_i^{n+1} < S_i$ then $E_i^{n+1} = 0$, else $E_i^{n+1} = 1$,
- if $E_i^n = 1$:
  if $A_i^{n+1} \geq S_i$ then $E_i^{n+1} = 1$, else $E_i^n = E_{i-1}^n \cdot E_{i+1}^n$.

Indeed, if $A_i^{n+1} \geq S_i$ it is clear that the state of the flow in the cell m_i becomes pressurized, on the other hand if $A_i^{n+1} < S_i$ in a mesh previously pressurized,

we do not know *a priori* if the new state is free surface ($\rho = \rho_0$ and the value of the wetted area is less than S_i) or pressurized (in depression, with $\rho < \rho_0$ and the value of the wetted area is equal to S_i: see Remark 5.4 and FIG. 10).
So far as we do not take into account complex phenomena such that entrapment of air pockets or cavitation and keeping in mind that the CFL condition ensures that a transition point crosses at most one mesh at each time step, we postulate that:

1. if the state of the flow in the cell m_i is free surface at time t_n, its state at time t_{n+1} is only determined by the value of A_i^{n+1} and it cannot become in depression.

2. if the state of the flow in the cell m_i is pressurized at time t_n and if $A_i^{n+1} < S_i$, it becomes free surface if and only if at least one adjacent cell was free surface at time t_n. This is exactly the discrete version of the continuous $\dfrac{A}{\mathbf{S}}$ criterion in Remark 5.4 and displayed on FIG. 10.

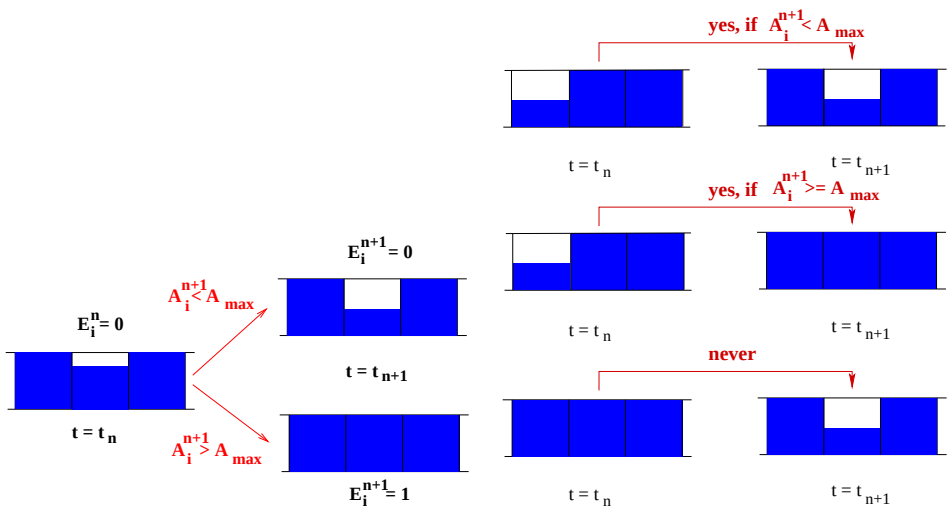

Figure 9: Update of the state E_i^{n+1} of the mesh m_i.

Remark 5.4 *As we do not take into account complex phenomena such that entrapment of air pockets, each connected component of the pressurized area is simply connected (see FIG. 10). Moreover, for each depression area D, its closure $\overline{D}$ is a strict subset of the pressurized set. It follows that when $A < S$ on each pressurized area, we observe a depression as displayed on FIG. 10. Moreover, we may also use a visual depression indicator given by the function $\dfrac{A}{\boldsymbol{S}}$: the case $\boldsymbol{S} = A$ corresponds to a free surface state while $\boldsymbol{S} > S$ to an overpressure state and $\boldsymbol{S} < S$ to a depression state. On FIG. 10, we draw the*

behavior of the interface speed w in the (X,t)-plane and the graph of the function $\frac{A}{S}$ at fixed time t_3.

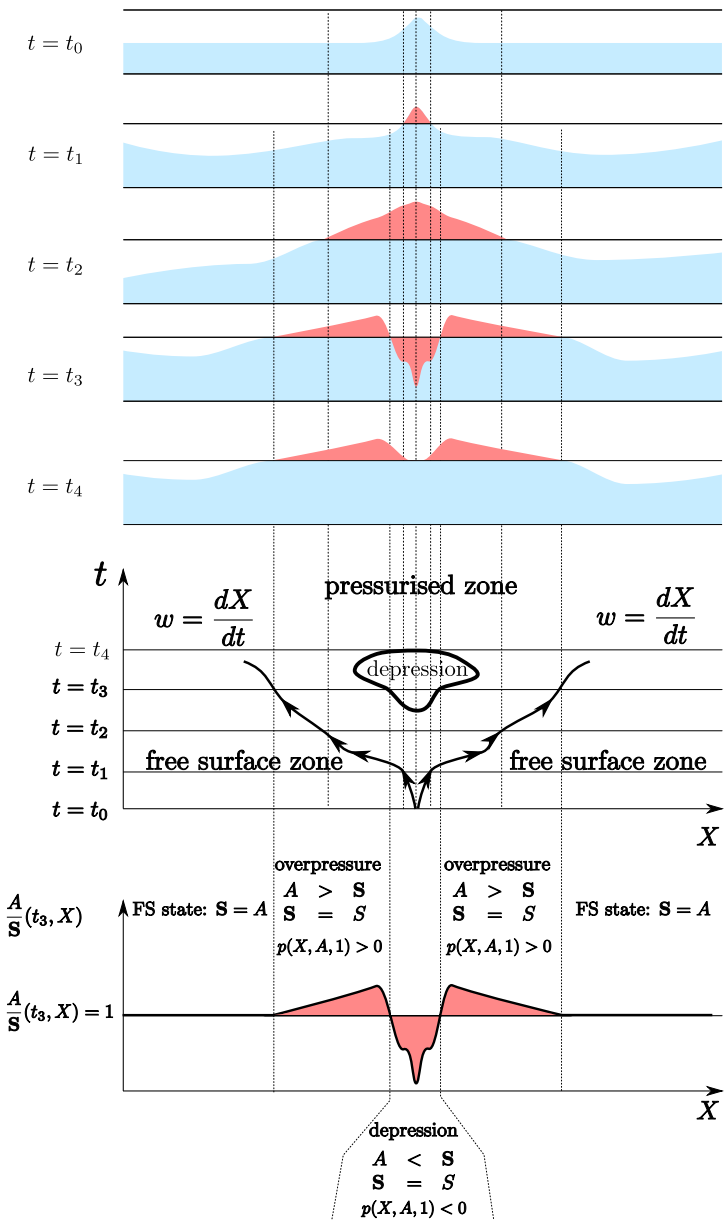

Figure 10: $\frac{A}{\mathbf{S}}$ depression indicator.

6 Remarks on still water steady state: an exactly well balanced scheme

This section is devoted to the construction of an exactly well-balanced scheme in the sense that it maintains perfectly the still water steady states. This scheme, noted EWBS, is obtained by a suitable definition of the convection matrix.
The numerical approximation of the **PFS**-model (21) reads:

$$A_i^{n+1} = A_i^n - \frac{\Delta t}{h_i}\left(Q_{i+1/2}^n - Q_{i-1/2}^n\right) \tag{41}$$

$$Q_i^{n+1} = Q_i^n - \frac{\Delta t}{h_i}\left(F_5(AM_{i+1/2}^n, Q_{i+1/2}^n) - F_5(AP_{i-1/2}^n, Q_{i-1/2}^n)\right) \tag{42}$$

where $Q_{i\pm 1/2}$ stands for $QMP_{i\pm 1/2}$ and $F_5(A,Q) = \dfrac{Q^2}{A} + c^2(A-\mathbf{S}) + g\, I_1(X,\mathbf{S})$.
For instance, in the subcritical case, the interface quantities reads:

$$\begin{aligned}
AM_{i+1/2}^n &= A_i^n + \frac{g\,\widetilde{A}_{i+1/2}^n}{2\,\widetilde{c}_{i+1/2}\,(\widetilde{c}_{i+1/2} - \widetilde{u}_{i+1/2}^n)}\,\psi_i^{i+1} \\
&\quad + \frac{\widetilde{u}_{i+1/2}^n + \widetilde{c}_{i+1/2}}{2\,\widetilde{c}_{i+1/2}}\,(A_{i+1}^n - A_i^n) - \frac{1}{2\,\widetilde{c}_{i+1/2}}\,(Q_{i+1}^n - Q_i^n) \\
Q_{i+1/2}^n &= Q_i^n - \frac{g\,\widetilde{A}_{i+1/2}^n}{2\,\widetilde{c}_{i+1/2}}\,\psi_i^{i+1} + \frac{\widetilde{u}_{i+1/2}^{n,2} - \widetilde{c}_{i+1/2}^2}{2\,\widetilde{c}_{i+1/2}}\,(A_{i+1}^n - A_i^n) \\
&\quad - \frac{\widetilde{u}_{i+1/2} - \widetilde{c}_{i+1/2}}{2\,\widetilde{c}_{i+1/2}}\,(Q_{i+1}^n - Q_i^n) \\
AP_{i+1/2}^n &= AM_{i+1/2}^n + \frac{g\,\widetilde{A}_{i+1/2}^n}{\widetilde{u}_{i+1/2}^{n,2} - \widetilde{c}_{i+1/2}^2}\,\psi_i^{i+1}
\end{aligned} \tag{43}$$

where the upwinded source term reads:

$$b_{i+1} - b_i + \mathcal{H}(\widetilde{\mathbf{S}}_{i+1/2}^n)(\cos\theta_{i+1} - \cos\theta_i) + \Psi(\widetilde{\mathbf{W}}i + 1/2^n)(S_{i+1} - S_i)$$

and $\widetilde{c}_{i+1/2}$ stands for $c(\widetilde{\mathbf{W}}_{i+1/2}^n)$ with

$$\widetilde{\mathbf{W}}_{i+1/2}^n = \left(\widetilde{b}_{i+1/2},\, \widetilde{\cos\theta}_{i+1/2},\, \widetilde{S}_{i+1/2},\, \widetilde{A}_{i+1/2}^n,\, \widetilde{Q}_{i+1/2}^n\right)$$

given by

$$\widetilde{b} = \frac{b_i + b_{i+1}}{2},\ \widetilde{\cos\theta} = \frac{\cos\theta_i + \cos\theta_{i+1}}{2},\ \widetilde{S} = \frac{S_i + S_{i+1}}{2},\ \widetilde{Q}_{i+1/2}^n = \frac{Q_i^n + Q_{i+1}^n}{2}, \tag{44}$$

and the approximation of $\widetilde{A}_{i+1/2}^n$ to be specified.
Starting from a discrete state (A_i^n, Q_i^n) at time t_n such that:

(H) let n such that: $\forall i$, $Q_i^n = 0$ and A_i^n satisfy the discrete still water steady state equation (according to Equation (24)):

$$c^2 \ln\left(\frac{A_{i+1}^n}{S_{i+1}}\right) + g\mathcal{H}(\mathbf{S}_{i+1}^n)\cos\theta_{i+1} + gb_{i+1} = c^2 \ln\left(\frac{A_i^n}{S_i}\right) + g\mathcal{H}(\mathbf{S}_i^n)\cos\theta_i + gb_i\,, \tag{45}$$

we will say that:

Definition 6.1

1. *The numerical scheme (41-42)-(44) for some approximations of the terms $\widetilde{A}_{i\pm1/2}^n$ is (k_A, k_Q) well-balanced (also denoted by (k_A, k_Q)-WB) if:*

   $$\forall i, \quad |A_i^{n+1} - A_i^n| = O((\max_{i\in\mathbb{Z}} h_i)^{k_A}) \text{ and } |Q_i^{n+1} - Q_i^n| = O((\max_{i\in\mathbb{Z}} h_i)^{k_Q})\,,$$

   with $k_A > 1$, $k_Q > 1$ the well-balanced order of the numerical scheme (41) and (42) respectively.

2. *The numerical scheme (41-42)-(44) for some approximations of the terms $\widetilde{A}_{i\pm1/2}^n$ is exactly well-balanced (also denoted by EWB) if:*

   $$\forall i, \quad |A_i^{n+1} - A_i^n| = 0 \text{ and } |Q_i^{n+1} - Q_i^n| = 0\,.$$

We will denote by (k_A, k_Q)-WBS the (k_A, k_Q) well-balanced scheme and EWBS the exactly well-balanced scheme.

(SF) In the rest of this paper, we assume $h_i = \Delta X$ constant, the radius R and b are given affine functions, the angle θ is constant which implies that the jumps across the interface $X_{i+1/2}$: $\Delta R_{i+1/2} = R_{i+1} - R_i = \Delta R$, $\Delta b_{i+1/2} = b_{i+1} - b_i = \Delta b$ are constant and $\Delta\cos\theta_{i+1/2}$ is null.

Then under this simplified framework, we show that:

Theorem 6.1

1. - *The numerical scheme (41-42)-(44) with the classical choice*

     $$\widetilde{A}_{i+1/2}^n = \frac{A_i^n + A_{i+1}^n}{2} \tag{46}$$

     and non constant section S is not well-balanced in the sense of Definition 6.1 (we have $k_Q = 1$).
   - *For constant section and $Z = 0$, the numerical scheme (41-42)-(44) with (46) is EWB.*

2. *Under a suitable choice of $\widetilde{A}_{i\pm1/2}^n$, the numerical scheme (41-42)-(44) is EWB.*

The following section deals with the numerical scheme with $\widetilde{A}_{i+1/2}^n$ defined as (46) where we show the first point of Theorem 6.1. The second point is studied in Section 6.2 where a convenient definition of $\widetilde{A}_{i+1/2}^n$ leads to an EWBS.

6.1 Still water steady state and the classical approximation

The simpler choice of definition for the convection matrix $D(\widetilde{\mathbf{W}})$ is the one obtained by the approximation of the mean value of the Roe matrix $D_{Roe}(\mathbf{W}_l, \mathbf{W}_r) = \int_0^1 D(\mathbf{W}_r + (1-s)(\mathbf{W}_l - \mathbf{W}_r))\, ds$. This approximation is given by $\widetilde{D} = D(\widetilde{\mathbf{W}}) = D\left(\dfrac{\mathbf{W}_l + \mathbf{W}_r}{2}\right)$ that we call "the classical approximation". Thus, defining $\widetilde{A}^n_{i+1/2}$ as follows:

$$\widetilde{A}^n_{i+1/2} = \frac{A^n_i + A^n_{i+1}}{2}$$

provides the classical approximation. But, it is not suitable to preserve the still water steady state: we will see that the numerical scheme (41-42)-(44) with (46) defines a non well-balanced scheme in the sense of Definition (6.1) since $k_Q = 1$. To this end, let us assume **(H)** and **(SF)** at time t_n, Equations (43) read for every i:

$$\begin{aligned}
AM^n_{i+1/2} &= A^n_i + \frac{g\,\widetilde{A}^n_{i+1/2}}{2\,\widetilde{c}^2_{i+1/2}}\,\psi^{i+1}_i + \frac{\Delta A^n_{i+1/2}}{2} \\
Q^n_{i+1/2} &= -\frac{g\,\widetilde{A}^n_{i+1/2}}{2\,\widetilde{c}_{i+1/2}}\,\psi^{i+1}_i - \widetilde{c}_{i+1/2}\frac{\Delta A^n_{i+1/2}}{2} \quad . \qquad (47) \\
AP^n_{i+1/2} &= AM^n_{i+1/2} - \frac{g\,\widetilde{A}^n_{i+1/2}}{\widetilde{c}^2_{i+1/2}}\,\psi^{i+1}_i
\end{aligned}$$

Denoting $Q_{i+1/2} - Q_{i-1/2}$ by $\Delta Q_{i+1/2}$, we have:

$$\begin{aligned}
\Delta Q^n_{i+1/2} \;=\; & \frac{g}{2\,\widetilde{c}_{i-1/2}\,\widetilde{c}_{i+1/2}}\Big\{ \left(\psi^i_{i-1} - \psi^{i+1}_i\right)\widetilde{c}_{i+1/2}\,\widetilde{A}^n_{i-1/2} \\
& - \left(\widetilde{A}^n_{i+1/2} - \widetilde{A}^n_{i-1/2}\right)\widetilde{c}_{i+1/2}\,\psi^{i+1}_i \\
& + \left(\widetilde{c}_{i+1/2} - \widetilde{c}_{i-1/2}\right)\widetilde{A}^n_{i+1/2}\,\psi^{i+1}_i \Big\} \\
& + \frac{\Delta A^n_{i+1/2}}{2}\left(\widetilde{c}_{i-1/2} - \widetilde{c}_{i+1/2}\right)
\end{aligned}$$

where

$$\widetilde{A}^n_{i+1/2} - \widetilde{A}^n_{i-1/2} \quad = \quad \Delta A^n_{i+1/2}$$

$$\psi^i_{i-1} - \psi^{i+1}_i \qquad = \quad \begin{cases} -\Delta b \quad \text{ if } E_i = 0 \\ \\ -\Delta b - \dfrac{g\,\cos\theta}{2}\Delta R \\ -\dfrac{c^2\,\Delta S_{i+1/2}}{S_{i-1/2}\,S_{i+1/2}} \\ \times\left(\Delta S_{i+1/2}\,\widetilde{A}^n_{i-1/2} - \Delta A^n_{i+1/2}\,S_{i-1/2}\right) \text{ if } E_i = 1 \end{cases} .$$

$$|\widetilde{c}_{i+1/2} - \widetilde{c}_{i-1/2}| \qquad \begin{cases} \leqslant & C\Delta X \text{ if } E_i = 0 \text{ (for some constant } C) \\ = & 0 \text{ if } E_i = 1 \text{ (since } \widetilde{c}_{i+1/2} = \widetilde{c}_{i-1/2} = c) \end{cases}$$

Denoting then

$$M = \max\left(\max_i\left(\widetilde{c}_{i+1/2}\,\widetilde{A}^n_{i-1/2}\right), \max_i\left(\widetilde{c}_{i+1/2}\,|\psi^{i+1}_i|\right), \max_i\left(\widetilde{A}^n_{i+1/2}\,|\psi^{i+1}_i|\right), C\right)$$

and observing that

$$\forall i,\, O(\Delta R) = O(\Delta S_{i+1/2}) = O(\Delta A^n_{i+1/2}) = O(\Delta X)$$

and

$$O(\widetilde{c}_{i+1/2}\,\widetilde{c}_{i-1/2}) = O(S_{i+1/2}\,S_{i-1/2}) = O(1)\,,$$

we deduce:

$$|\Delta Q^n_{i+1/2}| \leqslant M\Delta x^2\,.$$

It follows that:

$$|A^{n+1}_i - A^n_i| = O(\Delta X^2)\,.$$

Then, we denote $F_5(AM^n_{i+1/2}, Q^n_{i+1/2}) - F_5(AP^n_{i-1/2}, Q^n_{i-1/2})$ by $\Delta F = T_1 + T_2$ with

$$T_1 = \frac{\left(AM^n_{i+1/2} - AP^n_{i-1/2}\right)\left(Q^n_{i+1/2}\right)^2 + AM^n_{i+1/2}\left(\left(Q^n_{i+1/2}\right)^2 - \left(Q^n_{i-1/2}\right)^2\right)}{AM^n_{i+1/2}\,AP^n_{i-1/2}}$$

and

$$T_2 = \begin{cases} g\cos\theta\left(I_1(X_{i+1/2,}, AM^n_{i+1/2}) - I_1(X_{i+1/2,}, AP^n_{i-1/2})\right) & \text{if} \quad E_i = 0 \\ \\ c^2(AM^n_{i+1/2} - AP^n_{i-1/2}) + c^2\Delta S_{i+1/2} & \text{if} \quad E_i = 1 \end{cases}$$

where $|\left(Q^n_{i+1/2}\right)^2 - \left(Q^n_{i-1/2}\right)^2| = O(\Delta X^3)$ and

$$AM^n_{i+1/2} - AP^n_{i-1/2} \quad = \quad \Delta A^n_{i+1/2} + \frac{g}{2}\left(\frac{\widetilde{A}^n_{i+1/2}\psi^{i+1}_i}{\widetilde{c}^2_{i+1/2}} + \frac{\widetilde{A}^n_{i-1/2}\psi^{i}_{i-1}}{\widetilde{c}^2_{i-1/2}}\right) \quad . \tag{48}$$

As the term $\left(\frac{\widetilde{A}^n_{i+1/2}\psi^{i+1}_i}{\widetilde{c}^2_{i+1/2}} + \frac{\widetilde{A}^n_{i-1/2}\psi^{i}_{i-1}}{\widetilde{c}^2_{i-1/2}}\right)$ is at least of order ΔX since

$$\psi^{i+1}_i = O(\Delta X),$$

we have:

$$|AM^n_{i+1/2} - AP^n_{i-1/2}| = O(\Delta X)\,.$$

It follows that :

$$|Q^{n+1}_i - Q^n_i| = O(\Delta X)\,.$$

Remark 6.1 *For constant section S and $Z = 0$, it is easy to see that the numerical scheme (41-42)-(44) with (46) is EWB.*

Although the scheme (41-42)-(44) with (46) have an order $k_Q = 1$ for non constant section, the still water steady state for the pressurized case is very well maintained for great value of the sonic speed c. But it is not the case for the free surface numerical scheme (see Fig. 16 with $\Delta X = 10^{-3}$, $b = 10^{-2}$, uniform pipe with diameter 1). We plot in Fig. 14 and Fig. 15 a still water steady state for two values of c for a given $\Delta X = 1$ (with $b = -0.9$): the absolute error obtained is 10^{-5} for $c = 30$ and 10^{-9} for $c = 200$. Indeed, let us consider, for the sake of simplicity, the case $S = cte$. At the continuous level, the still water steady state equation reads:

$$c^2 \ln(A) + gR\cos\theta + gb = cte.$$

With the hypothesis **(H)**, in particular using Equation (45), we write:

$$A^n_{i+1} = A^n_i \exp\left(-\frac{g}{c^2}\Delta b\right)\,.$$

Given ΔX, for great value of c, we can approximate A^n_{i+1} by:

$$A^n_{i+1} \approx A^n_i\left(1 - \frac{g}{c^2}\Delta b\right)\,.$$

Then, replacing the right hand-side of A^n_{i+1} in (48), we have

$$|AM^n_{i+1/2} - AP^n_{i-1/2}| = \, g\, A^n_i \frac{|\Delta b|}{c^2} = O\left(\frac{\Delta X}{c^2}\right)\,.$$

As we can see k_Q is always equal to 1 but the constant $\frac{1}{c^2}$ plays the role of a smoothing term which helps the scheme (41-42)-(44) with (46) to stabilize rapidly towards the equilibrium. Physically, c is approximatively 1400 (for a pressurized flow without air), thus $\frac{1}{c^2} \approx 1.9\,10^{-6}$. Since $c(A) \ll c$, this feature is not observed for the free surface numerical scheme.

6.2 An exactly well-balanced scheme

This section is devoted to the construction of an EWBS. We have seen in Subsection 6.1 that the classical approximation of with $\widetilde{A}^n_{i\pm1/2}$ (46) is not appropriate to preserve the still water steady state. Thus, we have to find a suitable definition for $\widetilde{A}^n_{i\pm1/2}$ to obtain an exactly well-balanced scheme. For this purpose, let us assume **(SF)** and start with :
at the discrete level, the still water steady state is perfectly maintained (see Fig. 11): it exists n such that for every i, if $Q^n_i = 0$ and $\forall i$,

A1: $c^2 \ln\left(\dfrac{A^n_{i+1}}{S_{i+1}}\right) + g\mathcal{H}(\mathbf{S}^n_{i+1})\cos\theta + gb_{i+1} = c^2 \ln\left(\dfrac{A^n_i}{S_i}\right) + g\mathcal{H}(\mathbf{S}^n_i)\cos\theta + gb_i,$

A2: $AM^n_{i+1/2} = AP^n_{i-1/2},$

A3: $Q^n_{i+1/2} = Q^n_{i-1/2},$

then, for all $l > n$ the conditions A1, A2 and A3 holds.

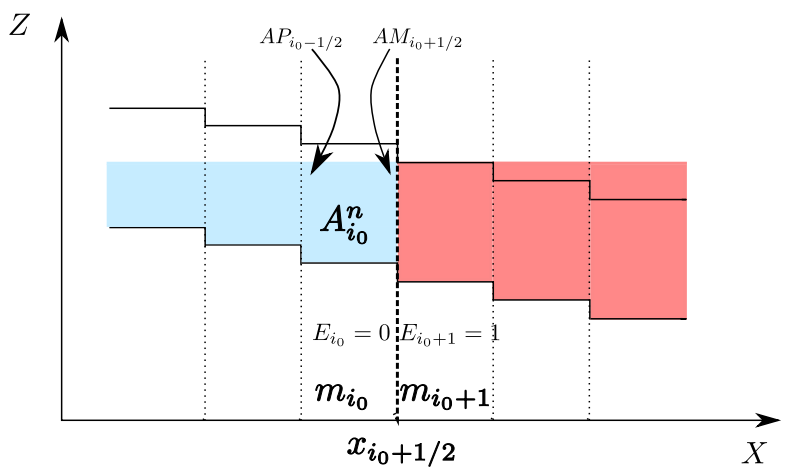

Figure 11: Discrete representation of the mixed free surface-pressurized still water steady state at time t^n.

The condition A2 is satisfied if and only if

$$AM^n_{i+1/2} - AP^n_{i-1/2} = \Delta A^n_{i+1/2} + \frac{g}{2}\left(\frac{\widetilde{A}^n_{i+1/2}\psi^{i+1}_i}{\widetilde{c}^2_{i+1/2}} + \frac{\widetilde{A}^n_{i-1/2}\psi^i_{i-1}}{\widetilde{c}^2_{i-1/2}}\right) = 0\,. \quad (49)$$

The condition A3 is satisfied if and only if

$$\Delta Q^n_{i+1/2} = \frac{g}{2}\left\{\frac{\widetilde{A}^n_{i-1/2}\,\psi^i_{i-1}}{\widetilde{c}_{i-1/2}} - \frac{\widetilde{A}^n_{i+1/2}\,\psi^{i+1}_i}{\widetilde{c}_{i+1/2}}\right\} + \frac{\Delta A^n_{i+1/2}}{2}\left(\widetilde{c}_{i-1/2} - \widetilde{c}_{i+1/2}\right) = 0\,. \quad (50)$$

The condition A1 is satisfied for pressurized flows if and only if

$$A_{i+1}^n = A_i^n \frac{S_{i+1}}{S_i} \exp\left(-\frac{g}{c^2}\left(\Delta b + \Delta R \cos\theta\right)\right) . \tag{51}$$

The condition A1 is satisfied for free surface flows if and only if

$$h_{i+1}^n = \frac{h_i^n \cos\theta - \Delta b}{\cos\theta} . \tag{52}$$

For circular cross-section pipe, A_{i+1}^n is computed by:

$$A_{i+1}^n = \frac{R_{i+1}^2}{2}\left(\omega_{i+1} - \sin(\omega_{i+1})\right) \tag{53}$$

with $\omega_{i+1} = 2\left(\pi - \arccos\left(\frac{h_{i+1}}{R_{i+1}}\right)\right)$ is the angle displayed on Fig. 12.

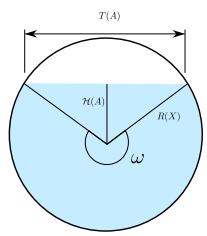

Figure 12: angle ω

Thus, the discrete still water steady state is perfectly maintained if and only if, $(\widetilde{A}_{i-1/2}^n, \widetilde{A}_{i+1/2}^n)$ is the solution of the non-linear system:

$$\left\{\begin{array}{rcl} 0 & = & \Delta A_{i+1/2}^n + \frac{g}{2}\left(\frac{\widetilde{A}_{i+1/2}^n \psi_i^{i+1}}{\widetilde{c}_{i+1/2}^2} + \frac{\widetilde{A}_{i-1/2}^n \psi_{i-1}^i}{\widetilde{c}_{i-1/2}^2}\right) \\ 0 & = & \frac{g}{2}\left\{\frac{\widetilde{A}_{i-1/2}^n\, \psi_{i-1}^i}{\widetilde{c}_{i-1/2}} - \frac{\widetilde{A}_{i+1/2}^n\, \psi_i^{i+1}}{\widetilde{c}_{i+1/2}}\right\} + \frac{\Delta A_{i+1/2}^n}{2}\left(\widetilde{c}_{i-1/2} - \widetilde{c}_{i+1/2}\right) \end{array}\right. \tag{54}$$

where we have replaced the expression of A_{i+1}^n in (49-50) by (51) for pressurized by (52) for free surface flows:

$$\Delta A_{i+1/2}^n = \left\{\begin{array}{ll} A_i^n\left(\frac{S_{i+1}}{S_i}\exp\left(-\frac{g}{c^2}\left(\Delta b + \Delta R\cos\theta\right)\right) - 1\right) & \text{if} \quad E_i = 0 \\ \mathcal{F}\left(\frac{h_i^n\cos\theta - \Delta b}{\cos\theta}\right) & \text{if} \quad E_i = 0 \end{array}\right. .$$

with $\mathcal{F} : h \mapsto \mathcal{F}(h) = A$. For circular pipe, $\mathcal{F}$ is given by (53).

Finally, the numerical scheme (41-42)-(44) with $\widetilde{A}^n_{i\pm 1/2}$ as the solution of the non linear system (54) defines an exactly well-balanced scheme.
For uniform pipe and pressurized flow, the previous system simply writes:

$$\left\{ \begin{array}{lcl} \Delta A^n_{i+1/2} + \dfrac{g\,\Delta Z}{2\,c^2}\left(\widetilde{A}^n_{i+1/2} + \widetilde{A}^n_{i-1/2}\right) & = & 0 \\ \\ \widetilde{A}^n_{i+1/2} & = & \widetilde{A}^n_{i-1/2} \end{array} \right. .$$

The solution is easily obtained by:

$$\widetilde{A}^n_{i+1/2} = -\frac{c^2}{g}\frac{\Delta A^n_{i+1/2}}{\Delta b} = -\frac{c^2}{g}\frac{A^n_i\left(\exp\left(-\frac{g}{c^2}\Delta b\right) - 1\right)}{\Delta b}. \tag{55}$$

Let us also remark that using the relation $A^n_i = A^n_{i+1}\exp\left(\frac{g}{c^2}\Delta b\right)$, we have:

$$\widetilde{A}^n_{i+1/2} = -\frac{c^2}{g}\frac{\Delta A^n_{i+1/2}}{\Delta b} = -\frac{c^2}{g}\frac{A^n_{i+1}\left(1 - \exp\left(\frac{g}{c^2}\Delta b\right)\right)}{\Delta b}. \tag{56}$$

It follows that $\widetilde{A}^n_{i+1/2}$ can be expressed as the mean value of (55) and (56) as follows:

$$\widetilde{A}^n_{i+1/2} = -\frac{c^2}{g\,\Delta b}\left\{\frac{A^n_{i+1}\left(1 - \exp\left(\frac{g}{c^2}\Delta b\right)\right) + A^n_i\left(\exp\left(-\frac{g}{c^2}\Delta b\right) - 1\right)}{2}\right\}.$$

For small ΔX, we have

$$\widetilde{A}^n_{i+1/2} \approx \frac{A^n_i + A^n_{i+1}}{2}.$$

It follows that the scheme (41-42)-(44) with (46) is the zero order approximation of the solution given by the EWBS.
The same analysis shows that the free surface numerical scheme with (46) is also the zero order approximation of the solution given by the EWBS.

On Fig. 14, Fig. 15, Fig. 16, we display the still water steady pressurized and free surface state computed by the EWBS and the scheme with the approximation (46). The steady state with the EWBS is numerically well preserved while as pointed out before (see Subsection 6.1) the classical approach is not convenient.
We also display an unsteady simulation on Fig. 17 where the results of the two methods are very well reproduced.

6.3 Remarks concerning mixed still water steady state

The previous sections deals with the well-balanced property of the numerical scheme (41-42)-(44) for free surface and pressurized flows. To use the well-balanced scheme developed in Subsections (6.1) and (6.2), we start from the

discrete representation of a mixed still water steady state (as displayed on Fig. 11). Assume that there exists i_0 such that all cells m_i on the left hand side of the interface $x_{i_0+1/2}$ are free surface while the other are pressurized:

$$\begin{cases} E_i = 0 & \text{if} \quad i \leqslant i_0 \\ E_i = 1 & \text{if} \quad i > i_0 \end{cases}.$$

The interface $x_{i_0+1/2}$ is such that the speed of propagation of the interface is null: $w^n_{i_0+1/2} = \dfrac{Q^n_{i+1} - Q^n_i}{A^n_{i+1} - A^n_i} = 0$ (see Fig. 13). Therefore, $\mathbf{UM} = \mathbf{U}^-$ and $\mathbf{UP} = \mathbf{U}^+$.

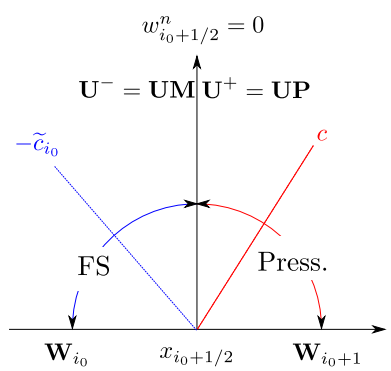

Figure 13: Mixed free surface-pressurized still water steady state

For example on Fig. 13, we apply the free surface numerical scheme on the left hand side of the interface and the pressurized one on the right cells . As the EWBS preserves the pressurized and free surface still water steady state, it also preserves the mixed still water steady state.

7 Numerical tests

The numerical validation for pipes with constant section and slope has been previously studied by two of the authors in [7, 8] and thus are not presented in this paper. Since experimental data for mixed flows in any pipe are not available, we focus on the behavior of our method for several circular cross-section contracting and expanding pipe. Notice that, the equivalent pipe method is not relevant for the mixed flows as pointed out by [1, 29, 30] for instance.
The mixed flow case is numerically performed on a water hammer test. Starting from an horizontal free surface still water steady state, the water hammer occurs immediately after the increase of the upstream piezometric head while the downstream discharge is set to 0. The prescribed hydrograph produces a travelling wave which produces a pressurized state propagating from upstream to downstream end. Physically an trapped air pocket may appear: it is not

taken into account in the **PFS**-model. Actually, the trapped air pockets vanish or move; some parts of these pockets undergo condensation/vaporisation and others parts move and lead to a two phase flow. Consequently the sound speed decreases. As our model does not take into account these phenomena, the value of c is assumed to be constant. Moreover we should have to deal with the entrapment of air bubbles which have a non negligible effect (see [19, 27] for instance).

The numerical experiments are performed in the case of a 100 m long closed circular pipe at altitude $b_0 = 1\,m$ with 0 slope which corresponds to the elevation and slope of the main pipe axis (we have $Z = b(X) = 0, \forall X$). The Manning roughness coefficient is $1/K_s = 0.012\ s/m^{1/3}$. The simulation starts from a steady state as a free surface flow with a discharge $Q = 0\ m^3/s$. The upstream boundary condition is a prescribed hydrograph (see Fig. 19) while the downstream discharge is kept constant to $0\,m^3/s$ (as displayed on Fig. 19). We compare then the results obtained for uniform, contracting an expanding pipes. For each test, the parameters are the same except the downstream diameter: the upstream diameter is kept constant to $D = 1\,m$. The contracting pipe is chosen for $D = 0.6\,m$ and the expanding one for $D = 1.4\,m$ (where D denotes the downstream diameter). Let us recall that the zero water level corresponds to the main pipe axis. The piezometric head is defined as $z + p$:

$$\begin{cases} p = 2R + \dfrac{c^2\,(\rho - \rho_0)}{\rho_0\, g} \text{ if the flow is pressurized} \\ p = h \text{ the water height if the flow is free surface} \end{cases}$$

Results are then represented on Fig. 20. The sudden raise of the upstream piezometric level produces a pressurized state with a travelling wave. A water hammer is then observed since the downstream discharge is null. A careful analysis of the flow which is performed by the variable E or equivalently by $\dfrac{A}{\mathbf{S}}$ (see Remark 5.4 and Fig. 10) shows that after this transition point, the flow is pressurized but in depression which starts approximatively at time $19s$ for the contracting pipe, $24s$ for the uniform pipe and $28s$ for the expanding one. We display the piezometric line for different times around the depression time (see Fig. 21) and also the graph of the function $\dfrac{A}{\mathbf{S}}$ which confirm that the observed times correspond exactly to a depression state for each pipes (see Fig. 22).

We also observe a little smoothing effect and absorption due to the first order discretisation type.

8 Conclusion

We have derived a free surface and a pressurized model which have been coupled using a common set of variables and a suitable pressure law. We have thus obtained a mathematical model for unsteady mixed flows in non uniform water pipes, that we have called **PFS**-model. This model takes into account the local perturbation of the section and of the slope.

The **PFS** model is numerically solved by a VFRoe scheme using the interfacial upwind to include the source terms into the numerical fluxes. We have shown that the classical approximation of the convection matrix (the Roe matrix approximation) is not suitable to preserve the still water steady state (except for the pressurized case where the value of c helps the scheme to maintain this state). Moreover, we have proposed a manner to obtain an exactly well-balanced scheme.

As mentioned in [7] this numerical method with the classical approximation of the convection matrix, for constant section, reproduces correctly laboratory tests for uniform pipes and can deal with multiple points of transition between the two types of flows. As pointed out before, due to the lack of experimental data for non uniform pipes, we have only shown the behavior of the piezometric line which seems reasonable (at less no major difference was observed).

As a well-known feature on approximate Godunov scheme, the upwinding of the source terms may introduce stationary waves with a vanishing denominator when critical flows occurs i.e. $u \approx c$. Moreover, in its actual form, the presented numerical scheme is not able to deal with drying and flooding area. Nevertheless, it may be possible to introduce a cut-off function to avoid division by zero for each problems: critical stationary waves, drying area and flooding area. But it is not the better choice that we can propose, since, truncation of the wet area induces a loss of water mass leading to the non-conservativity of the mass. Nevertheless, at the present time, we are interested in a mathematical kinetic formulation of the **PFS** model and the construction of a numerical kinetic scheme that avoids all these drawbacks [6].

The next step is to take into account the air entrainment which may have non negligible effects on the behaviour of the piezometric head. A first approach has been derived in the case of perfect fluid and perfect gas modelised as a bilayer model based on the **PFS**-model [5].

Aknowlegments: The authors wish to thank the two referees for their careful reading of the first version of the article and useful remarks.

References

[1] A. Adamkowski. Analysis of transient flow in pipes with expanding or contracting sections. *ASME J. of Fluid Engineering*, 125:716–722, 2003.

[2] B. Alvarez-Samaniego and D. Lannes. Large time existence for 3D water-waves and asymptotics. *Invent. Math.*, 171(3):485–541, 2008.

[3] F. Bouchut, E.D. Fernández-Nieto, A. Mangeney, and P.-Y. Lagrée. On new erosion models of Savage-Hutter type for avalanches. *Acta Mech.*, 199:181–208, 2008.

[4] F. Bouchut, A. Mangeney-Castelnau, B. Perthame, and J.-P.Vilotte. A new model of Saint Venant and Savage-Hutter type for gravity driven shallow water flows. *C. R. Math. Acad. Sci. Paris*, 336(6):531–536, 2003.

[5] C. Bourdarias, M. Ersoy, and S. Gerbi. Air entrainment in transient flows in closed water pipes: a two-layer approach. *submitted, available at* `http://arxiv.org/abs/0910.0334`, 2009.

[6] C. Bourdarias, M. Ersoy, and S. Gerbi. A model for unsteady mixed flows in non uniform closed water pipes: a Full Kinetic Approach. *In preparation*, 2009.

[7] C. Bourdarias and S. Gerbi. A finite volume scheme for a model coupling free surface and pressurized flows in pipes. *J. Comp. Appl. Math.*, 209(1):109–131, 2007.

[8] C. Bourdarias and S. Gerbi. A conservative model for unsteady flows in deformable closed pipe and its implicit second order finite volume discretisation. *Computers & Fluids*, 37:1225–1237, 2008.

[9] C. Bourdarias, S. Gerbi, and M. Gisclon. A kinetic formulation for a model coupling free surface and pressurized flows in closed pipes. *J. Comp. Appl. Math.*, 218(2):522–531, 2008.

[10] M. Boutounet, L. Chupin, P. Noble, and J-P. Vila. Shallow water viscous flows for arbitrary topopgraphy. *Commun. Math. Sci.*, 6(1):29–55, 2008.

[11] D. Bresch and P. Noble. Mathematical justification of a shallow water model. *Methods Appl. Anal.*, 14(2):87–117, 2007.

[12] T. Buffard, T. Gallouët, and J.M. Hérard. A sequel to a rough Godunov scheme. application to real gases. *Computers and Fluids*, 31:813–847, 2000.

[13] H. Capart, X. Sillen, and Y. Zech. Numerical and experimental water transients in sewer pipes. *Journal of Hydraulic Research*, 35(5):659–672, 1997.

[14] Nguyen Trieu Dong. Sur une méthode numérique de calcul des écoulements non permanents soit à surface libre, soit en charge, soit partiellement à surface libre et partiellement en charge. *La Houille Blanche*, 2:149–158, 1990.

[15] Musandji Fuamba. Contribution on transient flow modelling in storm sewers. *Journal of Hydraulic Research*, 40(6):685–693, 2002.

[16] T. Gallouët, J.M. Hérard, and N. Seguin. Some approximate Godunov schemes to compute shallow-water equations with topography. *Computers and Fluids*, 32:479–513, 2003.

[17] J.-F. Gerbeau and B. Perthame. Derivation of viscous Saint-Venant system for laminar shallow water; numerical validation. *Discrete Cont. Dyn. Syst. Ser. B*, 1(1):89–102, 2001.

[18] J.M. Greenberg and A.Y. LeRoux. A well balanced scheme for the numerical processing of source terms in hyperbolic equation. *SIAM J. Numer. Anal.*, 33(1):1–16, 1996.

[19] M.A. Hamam and A. McCorquodale. Transient conditions in the transition from gravity to surcharged sewer flow. *Can. J. Civ. Eng.*, 9:189–196, 1982.

[20] F. Kerger, P. Archambeau, S. Erpicum, B. J. Dewals, and M. Pirotton. Improved one-dimensional numerical simulation of transient mixed flow in water pipe. In *Proceedings of 4th Int. Conf. on Advanced Computational Methods in Engineering Liege, Belgium.*, 2008.

[21] F. Kerger, P. Archambeau, S. Erpicum, B. J. Dewals, and M. Pirotton. Numerical simulation of highly transient mixed flow in sewer system. *La Houille Blanche*, 2009. to appear.

[22] F. Kerger, S. Detrembleur, P. Archambeau, S. Erpicum, B. J. Dewals, and M. Pirotton. An experimental analysis of effects induced by moving bodies in shallow water. In *Proceedings of 2nd Int. Junior Researcher and Engineer Workshop on Hydraulic Structures, Pisa, Italy.*, 2008.

[23] C-D. Levermore, M. Oliver, and Edriss S. Titi. Global well-posedness for models of shallow water in a basin with a varying bottom. *Indiana University Mathematics Journal.*, 45(2), 1996.

[24] F. Marche. Derivation of a new two-dimensional viscous shallow water model with varying topography, bottom friction and capillary effects. *European Journal of Mechanic. B, Fluids*, 26(1):49–63, 2007.

[25] P.L. Roe. Some contributions to the modelling of discontinuous flow. In B. E. Engquist, S. Osher, and R. C. J. Somerville, editors, *Large-scale computations in fluid mechanics. Part 2. Proceedings of the fifteenth AMS-SIAM summer seminar on applied mathematics held at Scripps Institution of Oceanography, La Jolla, Calif., June 27-July 8, 1983*, volume 22 of *Lectures in Applied Mathematics*, pages 163–193. American Mathematical Society, 1985.

[26] A. Y. Le Roux and M. N. Le Roux. Convergence d'un schéma à profils stationnaires pour les équations quasi linéaires du premier ordre avec termes sources. *C. R. Acad. Sci.*, Sér. I, Math. 333(7):703–706, 2001.

[27] C.S.S. Song. Two-phase flow hydraulic transient model for storm sewer systems. In *Second international conference on pressure surges*, pages 17–34, Bedford, England, 1976. BHRA Fluid engineering.

[28] C.S.S. Song, J.A. Cardle, and K.S. Leung. Transient mixed-flow models for storm sewers. *Journal of Hydraulic Engineering, ASCE*, 109(11):1487–1503, 1983.

[29] V.L. Streeter, E.B. Wylie, and K.W. Bedford. *Fluid Mechanics*. McGraw-Hill, 1998.

[30] E.B. Wylie and V.L. Streeter. *Fluid Transients*. McGraw-Hill, New York, 1978.

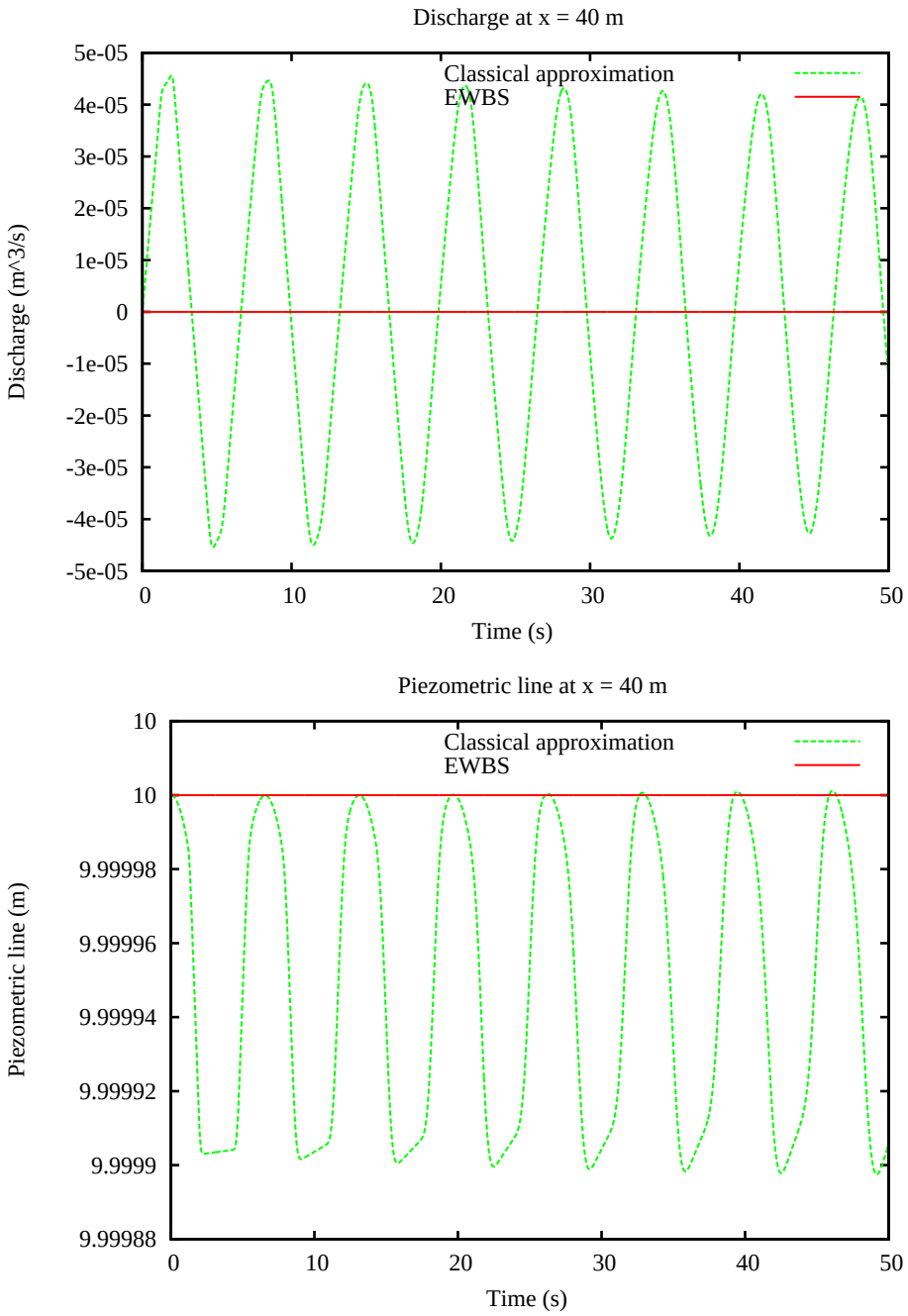

Figure 14: The numerical scheme (41-42)-(44) with (46) and the EWBS for pressurized still water steady state with $c = 30$.

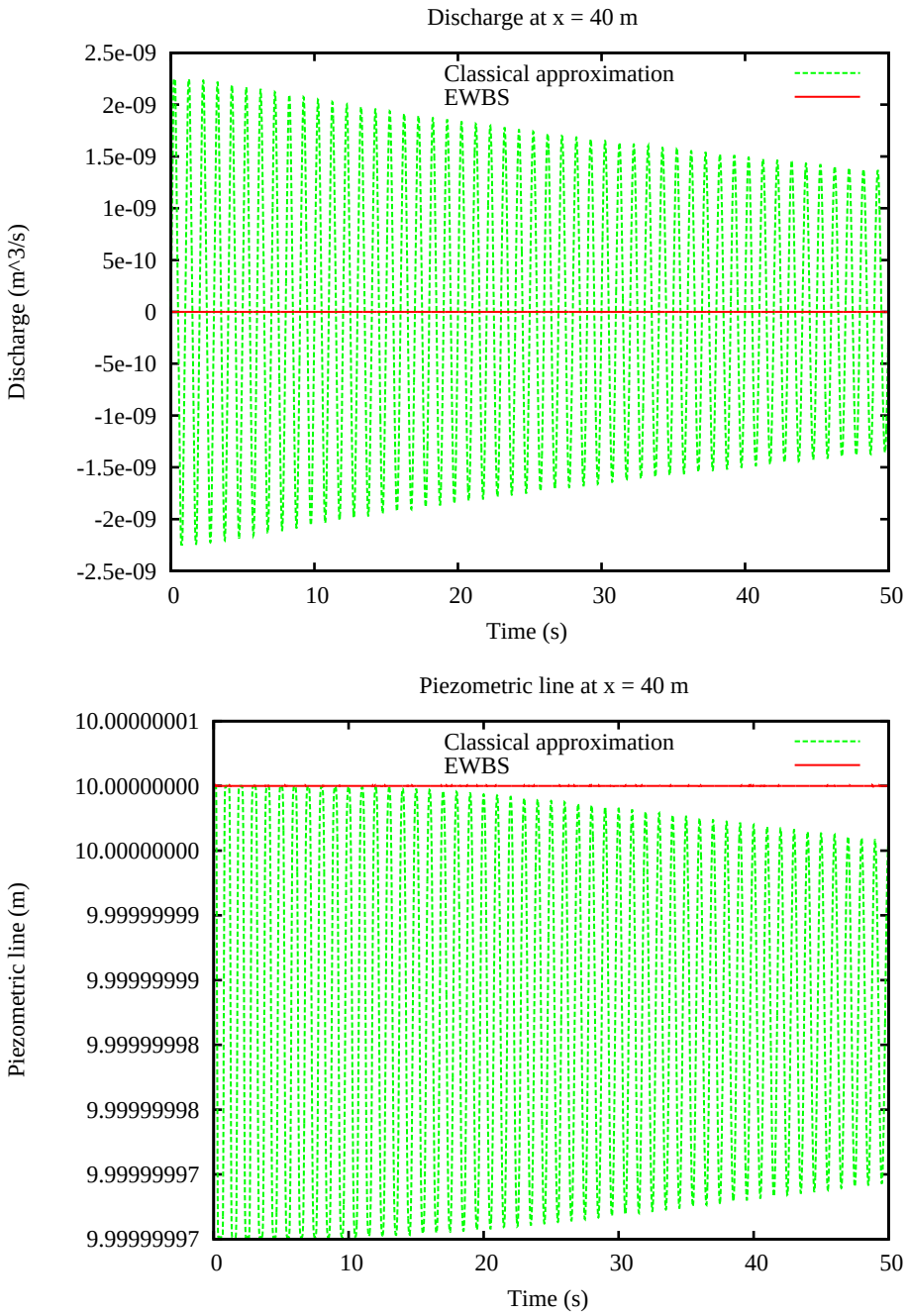

Figure 15: The numerical scheme (41-42)-(44) with (46) and the EWBS for pressurized still water steady state with $c = 200$.

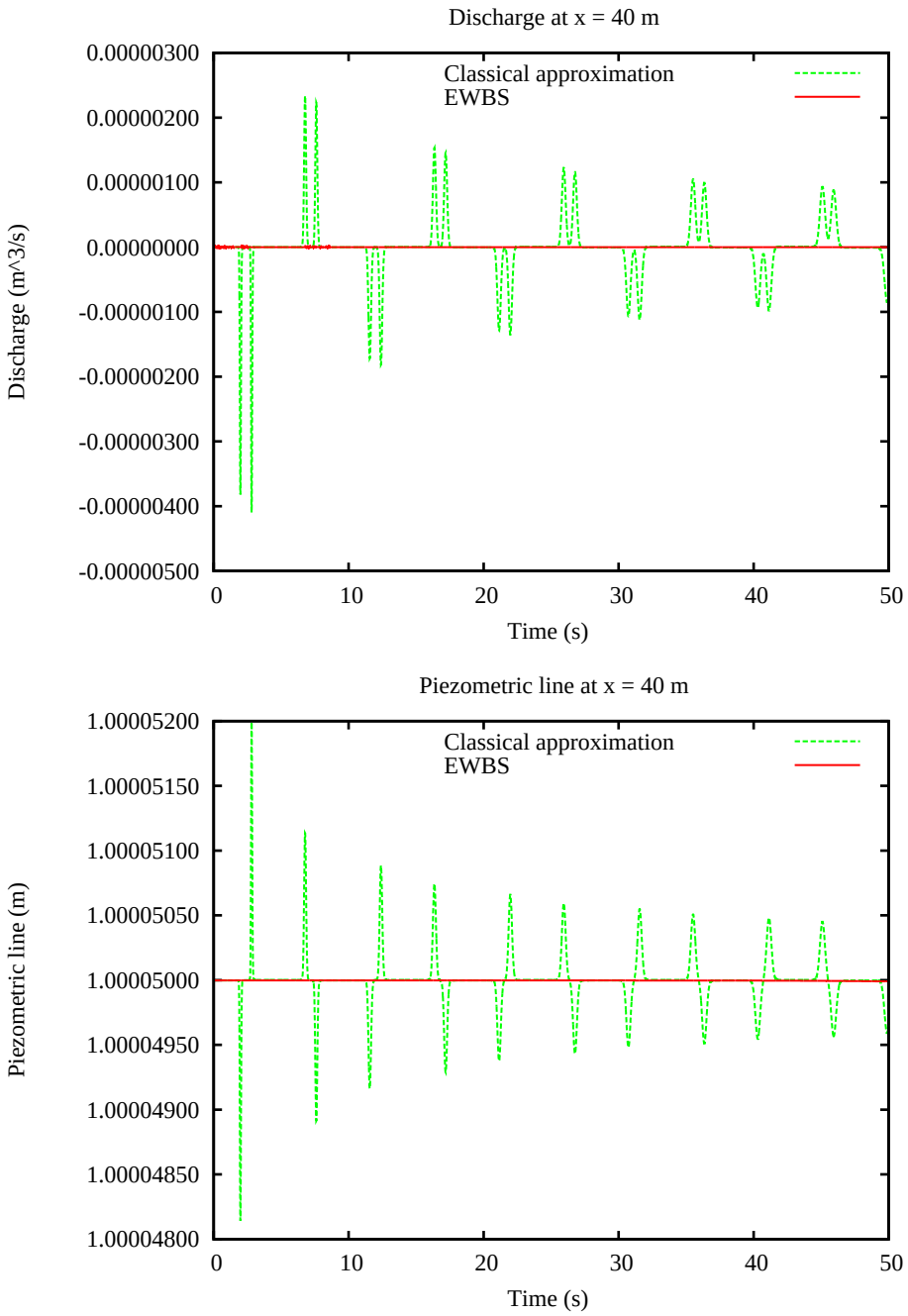

Figure 16: The numerical scheme (41-42)-(44) with (46) and the EWBS for free surface still water steady state.

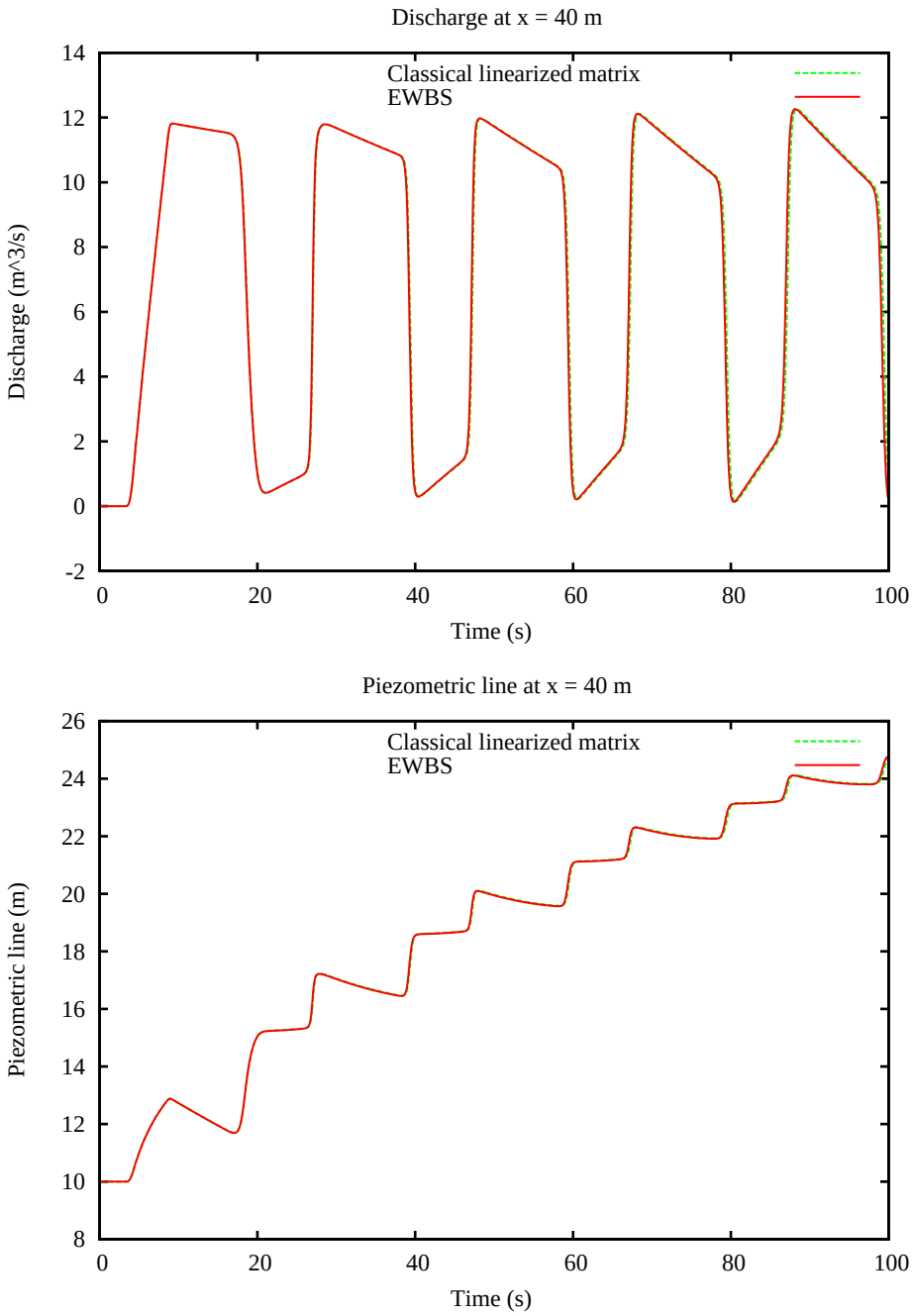

Figure 17: A non stationary test to compare the EWBS and the numerical scheme (41-42)-(44) with (46).

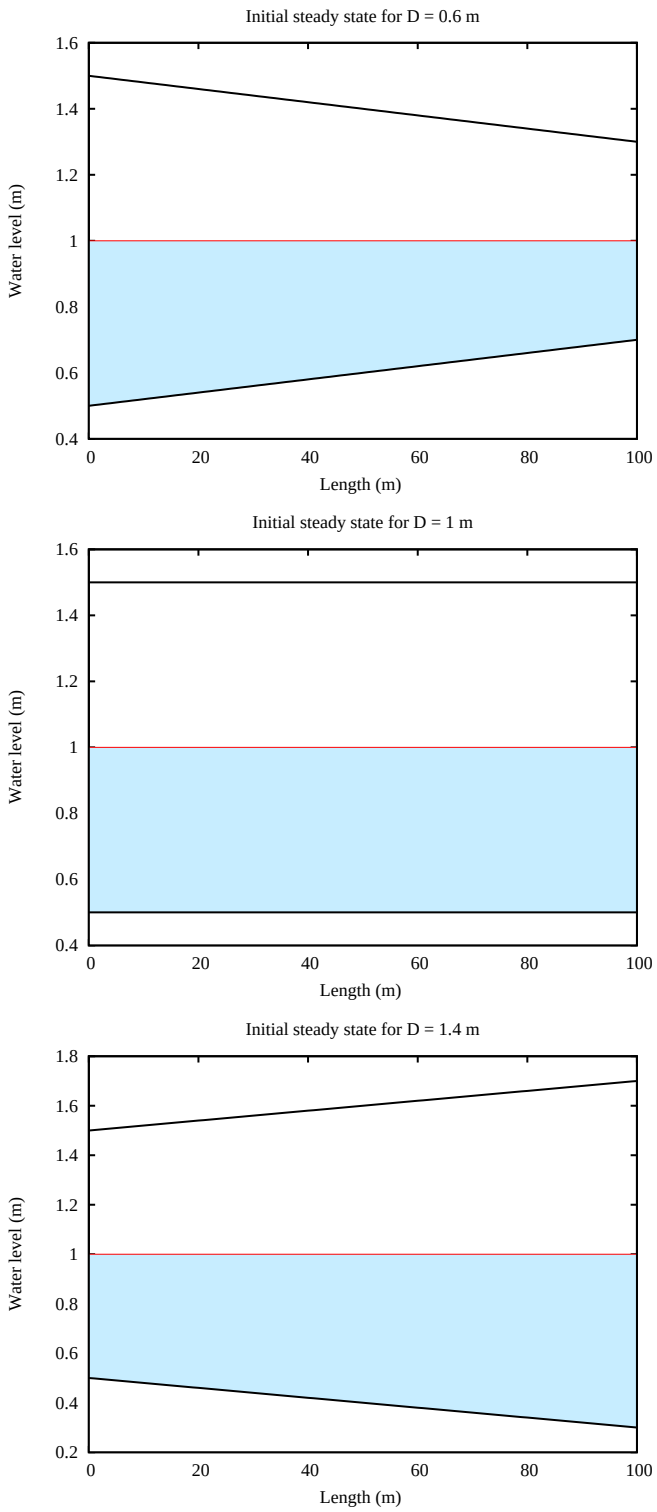

Figure 18: Initial still water steady state for contracting, uniform and expanding pipes .

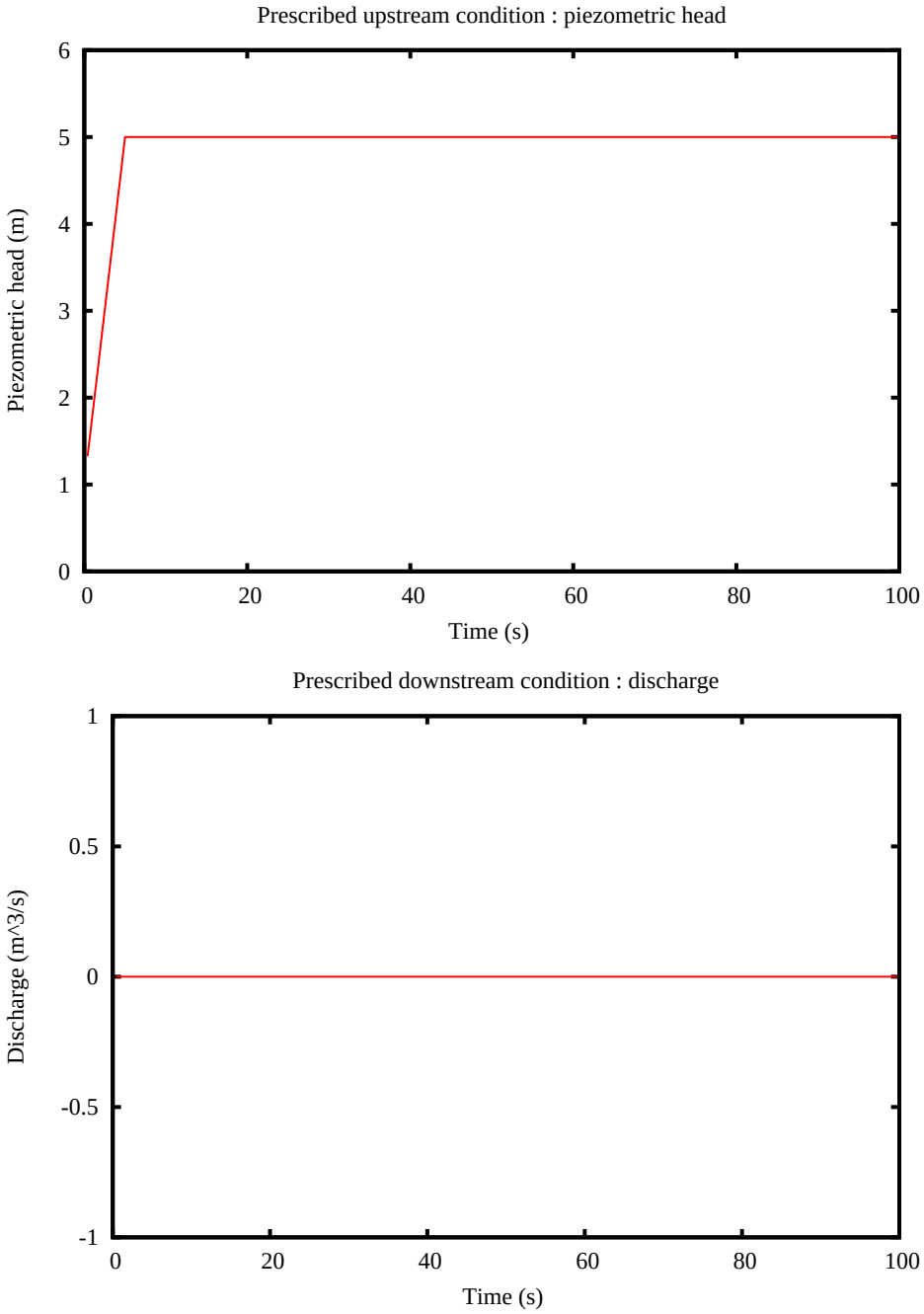

Figure 19: Boundary conditions.

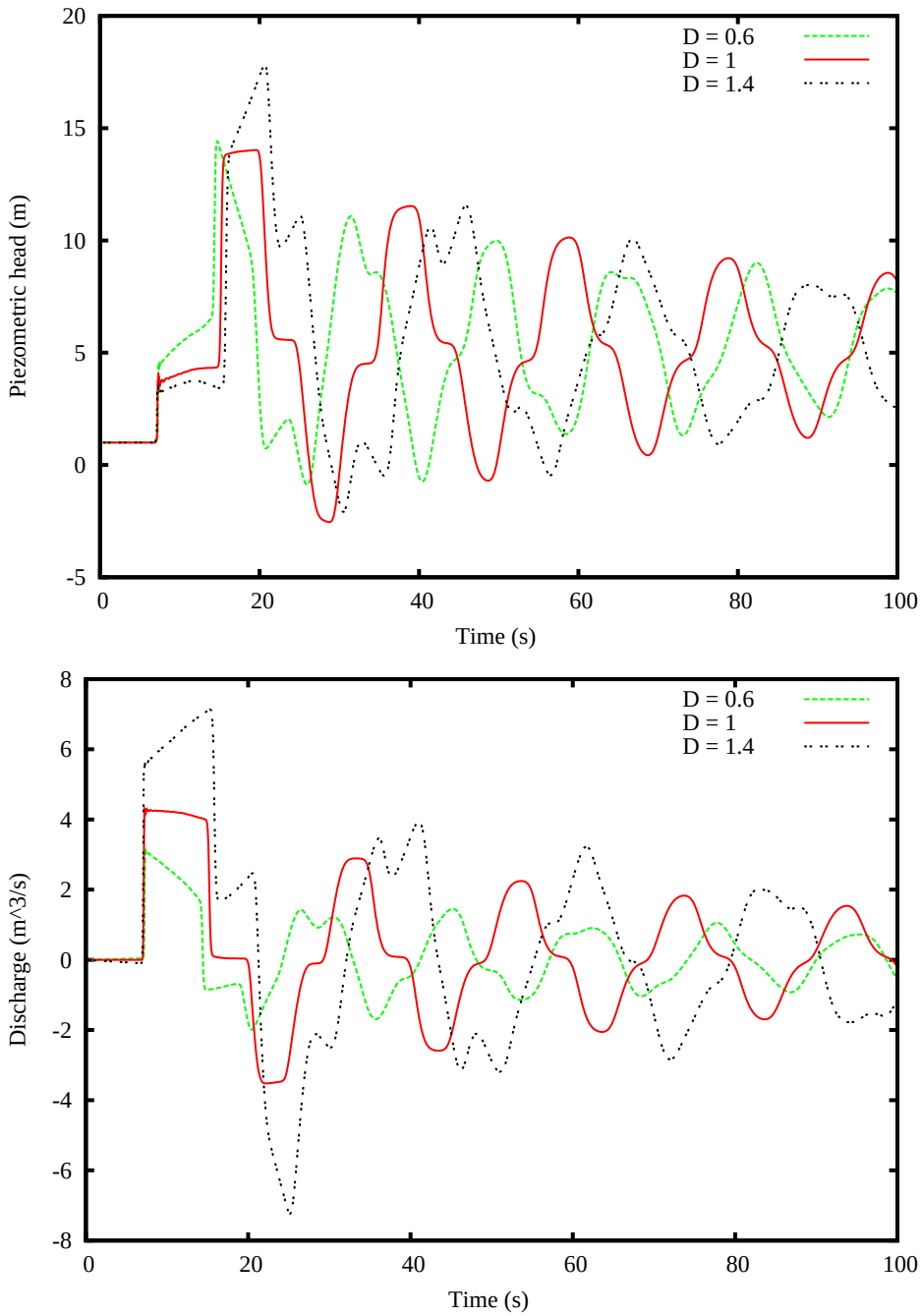

Figure 20: Piezometric head and discharge at $X = 50m$.

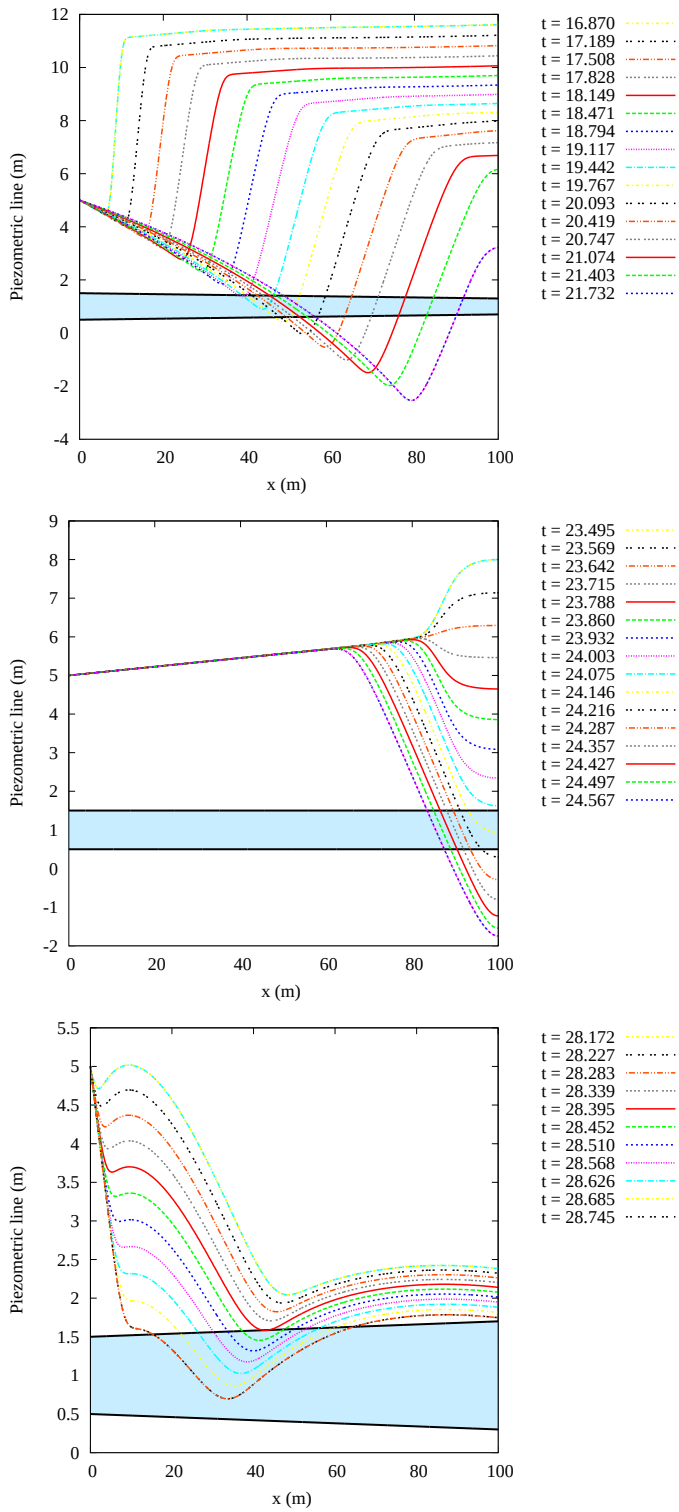

Figure 21: Observation of the depression localised approximatively at time $t = 19.117$ (contracting pipe), $t = 24.075$ (uniform pipe) and $t = 28.395$ (expanding pipe).

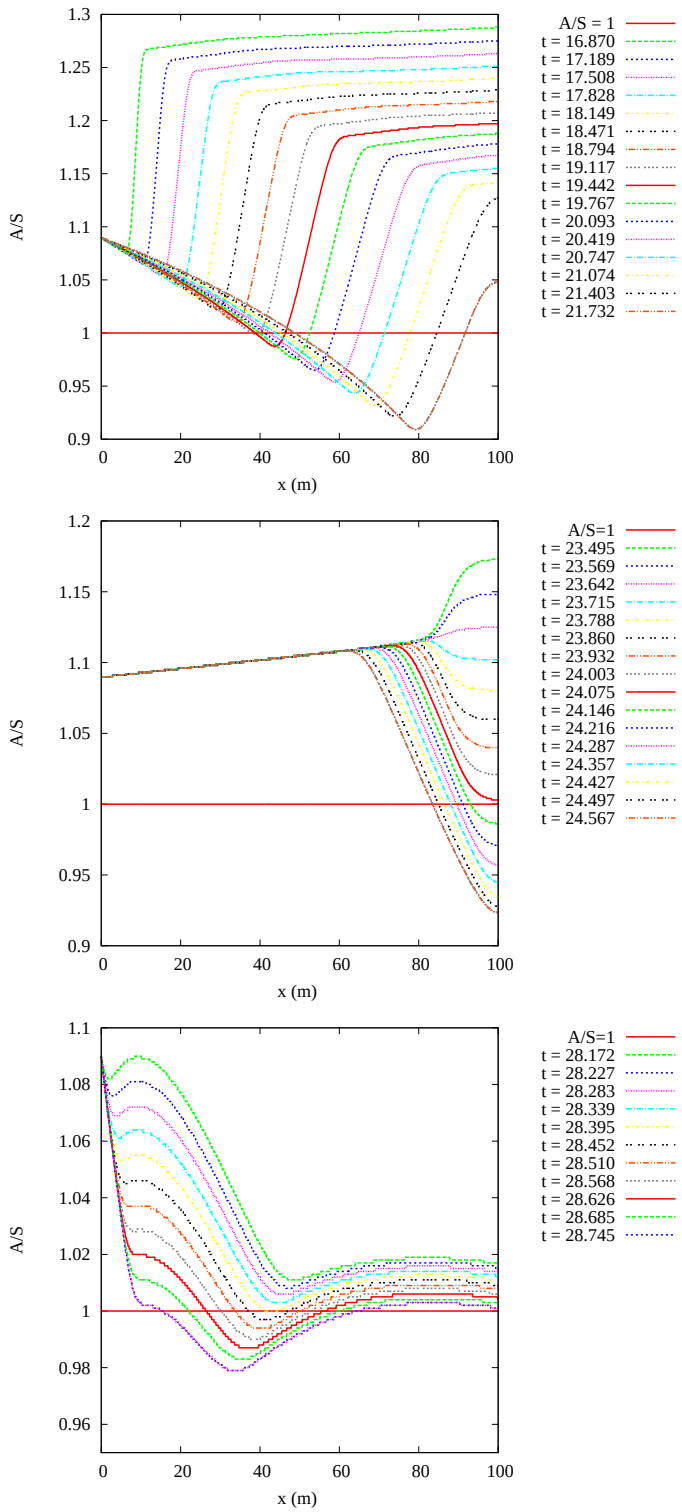

Figure 22: Observation of the depression localised approximatively at time $t = 19.117$ (contracting pipe), $t = 24.075$ (uniform pipe) and $t = 28.395$ (expanding pipe).

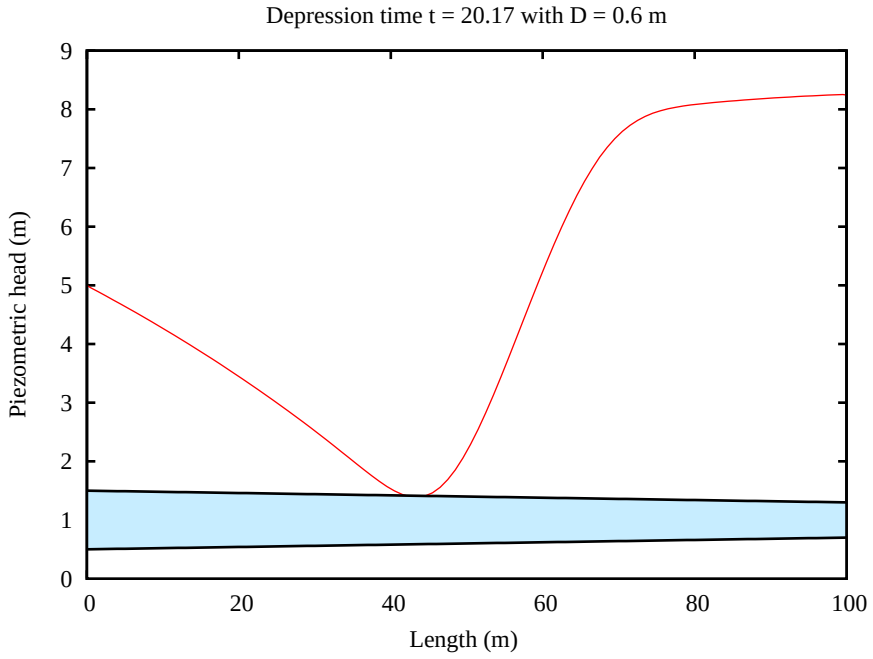
Depression time t = 20.17 with D = 0.6 m
Piezometric head (m)
Length (m)
0
1
2
3
4
5
6
7
8
9
0
20
40
60
80
100

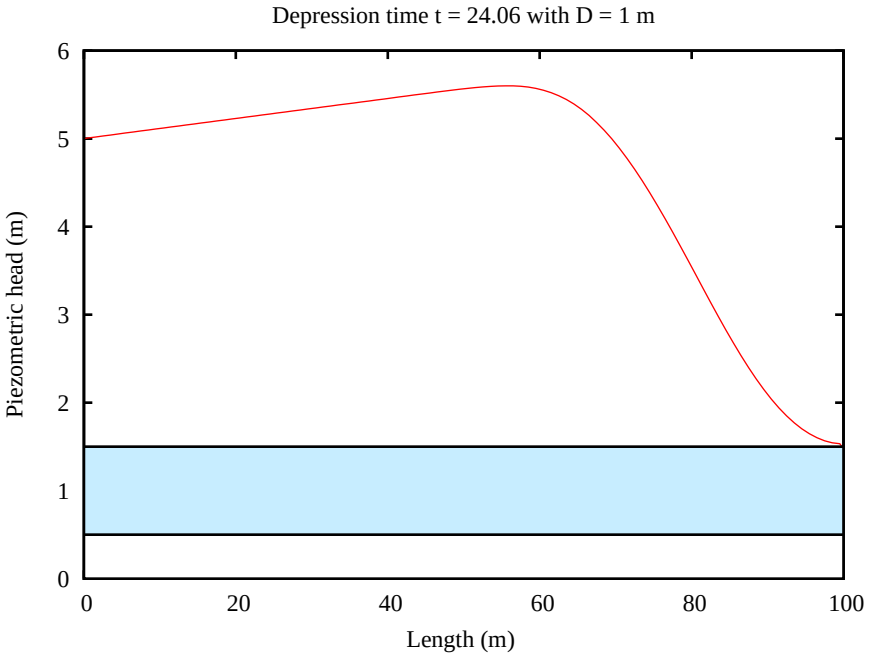
Depression time t = 24.06 with D = 1 m
Piezometric head (m)
Length (m)
0
1
2
3
4
5
6
0
20
40
60
80
100

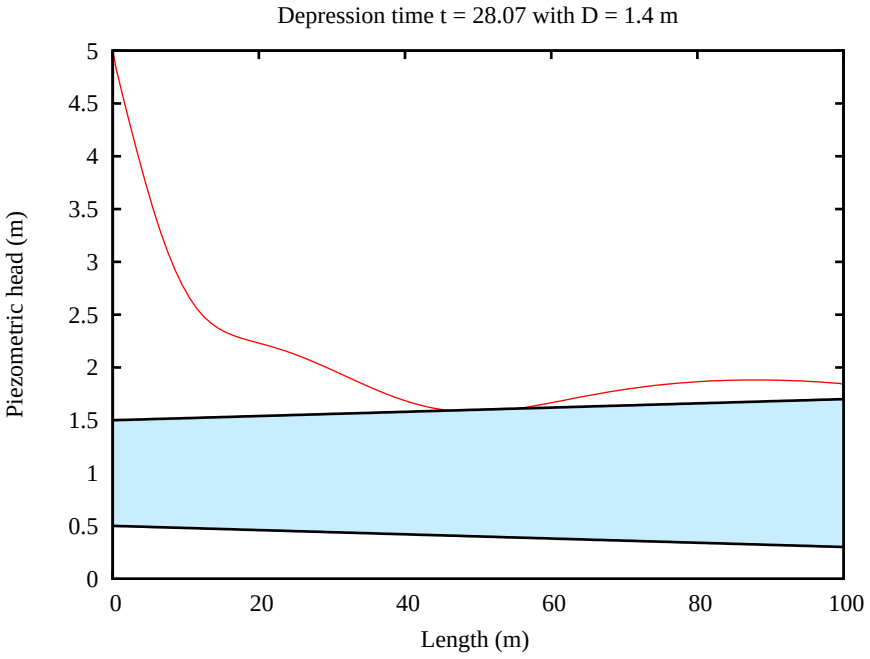
Depression time t = 28.07 with D = 1.4 m
Piezometric head (m)
Length (m)
0
0.5
1
1.5
2
2.5
3
3.5
4
4.5
5
0
20
40
60
80
100